Transverse-average field approach for the characterization of thin metamaterial slabs

Mário G. Silveirinha
Departamento de Engenharia Electrotécnica da Universidade de Coimbra, Instituto de Telecomunicações, Pólo II, 3030 Coimbra, Portugal

Carlos A. Fernandes
Instituto Superior Técnico-Instituto de Telecomunicações, Technical University of Lisbon, 1049-001 Lisbon, Portugal
(Received 28 May 2006; revised manuscript received 2 December 2006; published 26 March 2007)

The objective of this work is to investigate in which circumstances the scattering of electromagnetic waves by a thin metamaterial slab can be characterized using known effective parameters of the associated unbounded periodic bulk medium. It is proved that the classical approach or classical boundary conditions may become less accurate or incomplete if the size of inclusions is not significantly smaller than the wavelength. To circumvent this problem we demonstrate that the interaction of waves with metamaterial structures may in many cases with practical interest be conveniently described using a transverse averaged-field technique, and that this approach can be very accurate even for wide incident angles, evanescent waves, and for large and moderately large wavelengths.

DOI: 10.1103/PhysRevE.75.036613 PACS number(s): 42.70.Qs, 41.20.Jb, 78.20.−e, 78.68.+m

I. INTRODUCTION

The interaction of electromagnetic waves with complex artificial materials became a topic of great interest in the last few years [1,2]. The possibility of engineering new materials with unusual or not readily available in nature electromagnetic properties, is exciting because it may open new opportunities for enhanced and more compact devices or waveguides that may surpass the diffraction limit [3], and also because it may enable subwavelength imaging [4–6].

Typically, a metamaterial is formed by a periodic array of metallic-dielectric resonant inclusions, properly tailored in shape and size to provide a desired electromagnetic response. Since the size of the inclusions is relatively small in terms of the wavelength, it is possible and convenient to use homogenization methods to characterize the interaction of waves with these materials [7–12]. However, as pointed out in Ref. [7], even though in typical metamaterials the size of the inclusions is smaller than the wavelength, it is only marginally so, and thus it is quite possible that the actual granularity of the inclusions may not be neglected. Nevertheless, it is common in recent works to describe very thin metamaterial screens (most of the times with only one layer of inclusions) as bulk materials characterized by an effective permittivity and permeability, and to retrieve the effective parameters from measured or simulated *S*-parameter data [9,13]. But, is such a procedure really valid? What are its intrinsic limitations?

Recently, in Ref. [9] this problem was analyzed in detail and it was found that the effective parameters extracted from *S*-parameter data may be nonlocal and consequently may not satisfy conditions for passivity, causality, and absence of radiation losses. Indeed, as referred to in Ref. [9], these nonlocal parameters depend, in general, on the incident angle and may be different from the true local material parameters, particularly when the lattice constant is only marginally smaller than the wavelength.

Our goal here is twofold. The first objective is to study the scope of application of the classical homogenization approach (characterization of the slab using the bulk medium effective parameters defined for a three-dimensional (3D) periodic material) and of the classical boundary conditions (continuity of the tangential components of the macroscopic electromagnetic field) to the characterization of the scattering of waves by metamaterial slabs, and confirm that the classic approach may not be adequate when metamaterial screens are thin (in the extreme case with only one layer). The second objective is to demonstrate that it is possible, even when the classical approach fails, to use a modified homogenization procedure with modified boundary conditions to accurately characterize the reflection and transmission of waves by a thin metamaterial slab. It is proved that for some important geometries, this modified homogenization method only requires the knowledge of the effective parameters of the bulk medium, i.e., precisely the same information as the classical approach, being however, much more accurate and precise.

To this end, we will extend the theory introduced in our previous work [14], where we used the notion of transverse averaged fields to study the scattering of waves by a thin metamaterial slab formed by a set of crossed metallic wires. In Ref. [14], we found out that the average electromagnetic fields in the bulk medium may be very different from the actual fields at the interfaces, and that the identification of the metamaterial slab with the bulk medium was not possible. These results confirm that, in general, the extraction of the effective parameters from the *S*-parameter data may not be correct, even though for the geometry studied in Ref. [14], this problem may be blamed on the strong spatial dispersion characteristic of the crossed-wire mesh.

In order to clarify these issues, here we present a systematic study of the homogenization of arbitrary metamaterial slabs using a transverse averaged (TA)-field approach and theoretically derive the relation between this method and the classical approach. We will prove that in some circumstances the two methods are nearly equivalent, but that, in general, the transverse averaged-field approach is much more accurate because it takes into consideration the actual granularity

of the metamaterial. In addition, we will examine the boundary conditions at an interface and show that for some metamaterials an additional boundary condition (ABC) needs to be considered. The theoretical developments presented in this paper are extensively validated with full wave numerical simulations that demonstrate the application of our method to several canonical problems with practical interest, such as arrays of connected and nonconnected metallic wires, arrays of ε-negative (ENG) dielectric rods, and arrays of metallic patches.

It is important to point out that our objective in this work is not directly related with the extraction or calculation of the effective parameters of microstructured materials. Our perspective is completely different: the aim is to show that the interaction of waves with thin metamaterial screens may be characterized using the bulk medium effective parameters (effective ε and μ for 3D-periodic materials) using a modified homogenization approach based on the concept of TA fields. Or in other words, we prove that provided the effective parameters for a 3D-periodic lattice are known somehow, then these parameters may be sufficient to characterize the scattering of waves by slabs of the metamaterial, even in the extreme case in which the slab thickness is only one layer and the classical approach fails.

This paper is organized as follows. In Sec. II we briefly review the classical homogenization theory and discuss its scope of application to scattering problems. In Sec. III we introduce the TA-field approach, examine the problem of boundary conditions, and explain how the TA-field method can be applied to solve a scattering problem. In Sec. IV, we derive an exact relation between the TA fields and the classical macroscopic fields in a periodic electromagnetic crystal. Then, in Sec. V, it is demonstrated that for very long wavelengths the new TA-field method is equivalent to the classical approach. In Sec. VI, the proposed concepts are used to calculate the reflection characteristic of several metamaterial screens, and the results are compared with full wave simulations. Finally, in Sec. VII the conclusions are drawn.

In this work we assume that the fields are monochromatic with time variation $e^{+j\omega t}$. The microscopic electric and induction fields are denoted by $\mathbf{E}$ and $\mathbf{B}$, respectively. The macroscopic electric and induction fields (microscopic fields averaged over the volumetric unit cell) are denoted by $\mathbf{E}_{\mathrm{av}}$ and $\mathbf{B}_{\mathrm{av}}$, and the macroscopic magnetic field and the electric displacement vector are denoted by $\mathbf{H}_{\mathrm{av}}$ and $\mathbf{D}_{\mathrm{av}}$. Finally, the transverse averaged electric and induction fields (microscopic fields averaged over the cross section of the unit cell parallel to the pertinent interface) are denoted by $\mathbf{E}_{\mathrm{av},T}$ and $\mathbf{B}_{\mathrm{av},T}$. More precise definitions of the macroscopic fields and TA fields are given in Secs. II and III.

II. CLASSICAL METHOD

In this section, we briefly review the fundamentals of the classical homogenization formalism. We go over the definition of the effective parameters of bulk media (3D electromagnetic crystals), and discuss the validity of using these effective parameters to characterize the reflection of waves by metamaterial slabs.

A. Effective parameters of an electromagnetic crystal

The homogenization theory presented here follows closely that of our previous works [12,14] and is related with the classical Ewald-Bloch homogenization approach. We consider a periodic crystal invariant to translations along three primitive vectors, $\mathbf{a}_1$, $\mathbf{a}_2$, and $\mathbf{a}_3$ and characterized by the permittivity $\varepsilon=\varepsilon(\mathbf{r})$. The constituent materials are assumed nonmagnetic. The unit cell of the electromagnetic crystal is denoted by Ω, and its volume by V_{cell}. The microscopic fields $(\mathbf{E},\mathbf{B})$ verify the Maxwell equations

$$\nabla \times \mathbf{E} = -j\omega\mathbf{B}, \tag{1}$$

$$\nabla \times \frac{\mathbf{B}}{\mu_0} = j\omega\varepsilon(\mathbf{r})\mathbf{E}. \tag{2}$$

Let $(\mathbf{E},\mathbf{B})$ be a Floquet mode associated with the wave vector $\mathbf{k}=(k_x,k_y,k_z)$ and frequency ω. As in Refs. [14,15], we define the cell averaged (macroscopic) electric field as

$$\mathbf{E}_{\mathrm{av}} = \frac{1}{\mathbf{V}_{\mathrm{cell}}}\int_{\Omega} \mathbf{E}(\mathbf{r})e^{j\mathbf{k}\cdot\mathbf{r}}d^3\mathbf{r}, \tag{3}$$

and the field $\mathbf{B}_{\mathrm{av}}$ is defined similarly. Notice that the electromagnetic fields are averaged over the unit cell, i.e., over a volumetric region.

Multiplying both sides of Eq. (1) by $\exp(j\mathbf{k}\cdot\mathbf{r})$, integrating over Ω, and using the Floquet property it can be verified that

$$-\mathbf{k}\times\mathbf{E}_{\mathrm{av}} + \omega\mathbf{B}_{\mathrm{av}} = \mathbf{0}, \tag{4}$$

$$\omega\varepsilon_h\left(\mathbf{E}_{\mathrm{av}} + \frac{\mathbf{P}_g}{\varepsilon_h}\right) + \mathbf{k}\times\frac{\mathbf{B}_{\mathrm{av}}}{\mu_0} = \mathbf{0}, \tag{5}$$

where the *generalized* polarization vector is defined by

$$\mathbf{P}_g = \frac{1}{V_{\mathrm{cell}}j\omega}\int_{\Omega}\mathbf{J}_d e^{+j\mathbf{k}\cdot\mathbf{r}}d^3\mathbf{r}, \tag{6}$$

$\mathbf{J}_d=j\omega(\varepsilon-\varepsilon_h)\,\mathbf{E}$ is the polarization current, and ε_h is the permittivity of the host medium. If the unit cell contains perfectly electric conducting (PEC) inclusions, they can be modeled as regions with $\varepsilon=-\infty$. In that case the integrand of Eq. (6) becomes indeterminate because the electric field vanishes in the PEC regions. It is simple to verify that in those circumstances the generalized polarization vector can be alternatively written as

$$\mathbf{P}_g = \frac{1}{V_{\mathrm{cell}}j\omega}\left(\int_{A_c}\mathbf{J}_c e^{+j\mathbf{k}\cdot\mathbf{r}}ds + \int_{\Omega-V_c}\mathbf{J}_d e^{+j\mathbf{k}\cdot\mathbf{r}}d^3\mathbf{r}\right), \tag{7}$$

where V_c is the PEC region in the unit cell, A_c is the corresponding boundary surface, $\hat{\nu}$ is the outward unit vector normal to A_c, and $\mathbf{J}_c=\hat{\nu}\times\mathbf{B}/\mu_0$ is the density of current at the PEC inclusions.

The generalized polarization vector $\mathbf{P}_g$ describes the effect of not only the electric dipole moment of the cell, but also of the higher order multipoles, including the magnetic dipole moment. For very long wavelengths, the separation of the effects of mean and eddy microscopic currents yields the

following decomposition (see Appendix B for more details):

$$\mathbf{P}_g \approx \mathbf{P} - \frac{\mathbf{k}}{\omega} \times \mathbf{M}, \tag{8}$$

where $\mathbf{P}$ and $\mathbf{M}$ are, respectively, the classical polarization and magnetization vectors [16],

$$\mathbf{P} = \frac{1}{V_{\text{cell}} j\omega} \int_{\Omega} \mathbf{J}_d(\mathbf{r}) d^3\mathbf{r}, \tag{9}$$

$$\mathbf{M} = \frac{1}{2V_{\text{cell}}} \int_{\Omega} \mathbf{r} \times \mathbf{J}_d(\mathbf{r}) d^3\mathbf{r}. \tag{10}$$

Inserting Eq. (8) into Eq. (5) we obtain the well-known result for plane waves,

$$\omega \mathbf{D}_{\text{av}} + \mathbf{k} \times \mathbf{H}_{\text{av}} = \mathbf{0}, \tag{11}$$

where the (macroscopic) electric displacement $\mathbf{D}_{\text{av}} = \varepsilon_h \mathbf{E}_{\text{av}} + \mathbf{P}$, and the (macroscopic) magnetic field $\mathbf{H}_{\text{av}} = \mathbf{B}_{\text{av}}/\mu_0 - \mathbf{M}$, are defined consistently with classical theory. For local media, it is possible to introduce permittivity and permeability dyadics such that $\mathbf{D}_{\text{av}} = \bar{\bar{\varepsilon}}(\omega) \cdot \mathbf{E}_{\text{av}}$ and $\mathbf{B}_{\text{av}} = \bar{\bar{\mu}}(\omega) \cdot \mathbf{H}_{\text{av}}$. Then, using Eqs. (4) and (11) it is feasible to calculate the properties of plane waves (dispersion characteristic $\omega = \omega(\mathbf{k})$, polarization of the fields, etc.) that propagate in the bulk homogenized medium. The calculation of the effective parameters $\bar{\bar{\varepsilon}}$ and $\bar{\bar{\mu}}$ is outside the scope of this paper. Our objective here is to prove that if these parameters are known somehow, then they may be used to characterize the reflection of waves by thin metamaterial screens using a new TA-field approach. This will be the topic of Sec. III.

For future reference, we note that it is also possible to relate the generalized polarization vector $\mathbf{P}_g$ with the average electric field $\mathbf{E}_{\text{av}}$ by introducing a dielectric function $\bar{\bar{\varepsilon}}_{\text{eff}} = \bar{\bar{\varepsilon}}_{\text{eff}}(\omega, \mathbf{k})$ such that

$$\bar{\bar{\varepsilon}}_{\text{eff}} \cdot \mathbf{E}_{\text{av}} = \varepsilon_h \mathbf{E}_{\text{av}} + \mathbf{P}_g. \tag{12}$$

For the case in which the homogenized medium is local and characterized by permittivity and permeability tensors, it is straightforward to verify that [15]

$$\bar{\bar{\varepsilon}}_{\text{eff}}(\omega, \mathbf{k}) = \bar{\bar{\varepsilon}}(\omega) + \frac{\mathbf{k}}{\omega} \times [\bar{\bar{\mu}}^{-1}(\omega) - \bar{\bar{\mathbf{I}}}] \times \frac{\mathbf{k}}{\omega}, \tag{13}$$

where $\bar{\bar{\mathbf{I}}}$ is the identity dyadic. It is also possible to obtain a similar formula for the case in which the homogenized medium is bianisotropic [17]. Note that, in general, $\bar{\bar{\varepsilon}}_{\text{eff}}$ is a function of both frequency and wave vector. Substituting Eq. (12) into Eq. (5) we obtain that

$$\omega \bar{\bar{\varepsilon}}_{\text{eff}} \cdot \mathbf{E}_{\text{av}} + \mathbf{k} \times \frac{\mathbf{B}_{\text{av}}}{\mu_0} = \mathbf{0}. \tag{14}$$

which can also be used together with Eq. (4) to calculate the properties of plane wave solutions in the homogenized medium, as an alternative to Eq. (11). We note that it is always possible to define a dielectric function, $\bar{\bar{\varepsilon}}_{\text{eff}}$, consistent with Eq. (12), even when the homogenized medium is nonlocal (spatially dispersive), and the effective permeability loses its meaning [18].

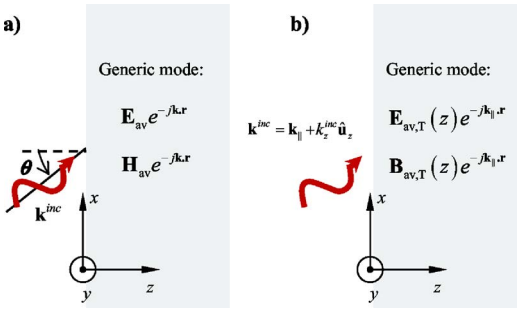

FIG. 1. (Color online) Solution of the scattering problem using a homogenization approach. (a) In the classical approach the fields inside the slab are a superimposition of the average fields in the infinite lattice and have plane wavelike properties. (b) In the TA-field approach the fields inside the metamaterial are taken equal to a superimposition of the transverse averaged electromagnetic modes of the infinite lattice.

The main motivation for introducing the dielectric function $\bar{\bar{\varepsilon}}_{\text{eff}}$, is that it allows one to describe in an unified manner the case in which the materials are characterized by strong spatial dispersion, the case in which the effect of higher order multipoles is non-negligible, and also, of course, the traditional case in which the medium can be described by an effective permittivity and permeability. For more details about the electrodynamics of spatially dispersive media the reader is referred to Refs. [15] and [18].

B. Scattering problem

Even though from a conceptual point of view it may be convenient to describe a metamaterial as a 3D periodic structure (e.g., to extract its effective parameters), all practical realizations have a finite number of inclusions. Nevertheless, since artificial materials are usually fabricated using planar technology, they can be regarded to a good approximation as an array of periodic screens. Typical metamaterial prototypes have, in general, a relatively small number of layers (1–4), in part because the fabrication of these complex structures is still a real challenge.

Here, we want to go over the problem of characterization of metamaterial screens using the effective parameters defined for the associated 3D-periodic electromagnetic crystal (bulk medium). To begin with, consider the geometry depicted in Fig. 1(a). It represents a generic metamaterial slab illuminated by a plane wave. It is assumed that the metamaterial slab corresponds to a truncated electromagnetic crystal (the slab consists of a finite number of layers). The wave vector of the incident wave is $\mathbf{k}^{\text{inc}} = \mathbf{k}_{\parallel} + \hat{\mathbf{u}}_z k_z^{\text{inc}}$, where the transverse wave vector is given by $\mathbf{k}_{\parallel} = (k_x, k_y, 0)$, and the wave number along the z direction is $k_z^{\text{inc}} = -j\sqrt{k_{\parallel}^2 - \omega^2 \varepsilon_0 \mu_0}$. Notice that for a propagating wave, we have that $k_{\parallel} = \frac{\omega}{c} \cos\theta$, where θ is the incident angle.

As is well known, the microscopic fields in the metamaterial slab are the superimposition of Floquet modes of the infinite lattice, with wave vector of the form $\mathbf{k}_n = \mathbf{k}_{\parallel} + k_{z,n}$ (i.e.,

the transverse component of the incident wave vector is preserved) [14]. In the long wavelength limit, only a few of the Floquet modes can propagate and thus, to a first approximation, it may be a good assumption to consider that these modes are sufficient to obtain an accurate representation of the fields in the metamaterial.

The classical homogenization theory is based precisely on such assumptions. In fact, in classical theory all Floquet modes are neglected, except those that can be described using the effective parameters of the bulk medium. The classical homogenization approach is summarized in Fig. 1(a). The fields inside the metamaterial slab are the superimposition of the average modal fields $(\mathbf{E}_{\mathrm{av}},\mathbf{H}_{\mathrm{av}})$ of the infinite lattice, and the classical boundary conditions (continuity of the tangential components of $\mathbf{E}_{\mathrm{av}}$ and $\mathbf{H}_{\mathrm{av}}$) are enforced at the interfaces. Note that average fields have plane-wave-like spatial variation inside the slab: $e^{-j\mathbf{k}\cdot\mathbf{r}}$. In particular, the variation of each mode along the z direction is of the form $e^{-jk_z z}$.

As discussed in the Introduction, for thin metamaterial slabs with thickness smaller than the characteristic transition layers, the classical approach may not be appropriate to solve the scattering problem. This problem becomes even more important if the wavelength of radiation is only moderately larger than the lattice constant. In fact, unlike natural materials in which the characteristic dimensions of the cell ($\sim$0.1 nm) are several orders of magnitude smaller than the wavelength, in typical microstructured materials the lattice constant is only ten times smaller than the wavelength.

In this work, we propose a modified homogenization procedure that helps solving the identified problems. The main idea is that the fields (associated with a Floquet mode) may vary considerably in the unit cell. Thus, at the interfaces (where the fields in the different regions are matched) the electromagnetic fields may be very different from the fields averaged over the unit cell $(\mathbf{E}_{\mathrm{av}},\mathbf{B}_{\mathrm{av}})$. It is clear that this may be a shortcoming. To circumvent these problems, in the next section we introduce the concept of TA fields and explain how such a concept can be used to characterize the scattering of waves by thin metamaterial slabs.

III. TRANSVERSE AVERAGED-FIELD METHOD

In this section, following the idea originally proposed in Ref. [14], we present an homogenization approach that is adequate to study the interaction of electromagnetic waves with metamaterial slabs. Unlike the classical homogenization methods, which were developed to characterize structures with a large number of layers or cells, the formalism introduced here can be applied to study both very thin metamaterial screens (with only one layer) or thick metamaterial slabs (with many layers). Later in the paper, we will discuss the connection between the two formalisms.

A. Definition and properties of transverse averaged fields

Let us consider a generic structure characterized by the permittivity $\epsilon=\epsilon(\mathbf{r})$ and invariant to translations (i.e., periodic) along the primitive vectors $\mathbf{a}_1$ and $\mathbf{a}_2$ (see Fig. 2). We suppose that the primitive vectors lie on the xoy plane (the

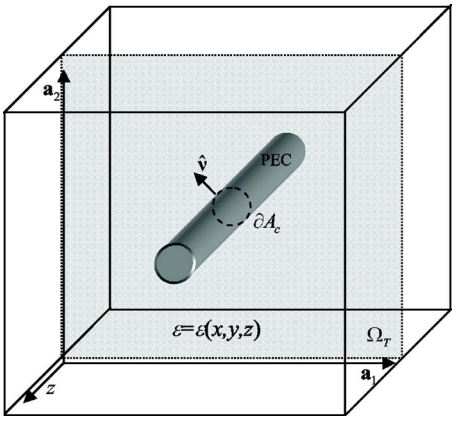

FIG. 2. (Color online) Geometry of the basic cell of a generic metamaterial. The structure is periodic along $\mathbf{a}_1$ and $\mathbf{a}_2$, but the geometry can be arbitrary along the z direction.

primitive vectors are not necessarily orthogonal). Note that unlike in Sec. II A the structure does not have to be periodic along the z direction. For each z=const. plane it is convenient to introduce the transverse unit cell $\Omega_T(z)=\{(0,0,z)+\alpha_1\mathbf{a}_1+\alpha_2\mathbf{a}_2:|\alpha_i|\leq\frac{1}{2}\}$.

It is convenient to regard the periodic structure as a stack (along the z direction) of different metamaterial layers (see Fig. 3). Each metamaterial layer is formed by an array of inclusions embedded in a host medium. Hence, we admit that permittivity of the host may vary from layer to layer, i.e., that $\varepsilon_h=\varepsilon_h(z)$.

As in Sec. II B, we suppose that an incoming plane wave with wave vector $\mathbf{k}^{\mathrm{inc}}=\mathbf{k}_{\|}+\hat{\mathbf{u}}_z k_z^{\mathrm{inc}}$, illuminates the metamaterial screen (Fig. 3). As is well known, the total microscopic fields $(\mathbf{E},\mathbf{B})$ have the Floquet-Bloch property, i.e., $(\mathbf{E},\mathbf{B})e^{j\mathbf{k}_{\|}\cdot\mathbf{r}}$ is periodic in the lattice.

Following Ref. [14], we define the transverse average (TA) electric field as

$$\mathbf{E}_{\mathrm{av},T}(z;\mathbf{k}_{\|})=\frac{1}{A_{\mathrm{cell}}}\int_{\Omega_T}\mathbf{E}(\mathbf{r})e^{j\mathbf{k}_{\|}\cdot\mathbf{r}}dxdy, \tag{15}$$

where $A_{\mathrm{cell}}=|\mathbf{a}_1\times\mathbf{a}_2|$ is the area of Ω_T. The field $\mathbf{B}_{\mathrm{av},T}$ is defined similarly. Note that the electromagnetic fields are

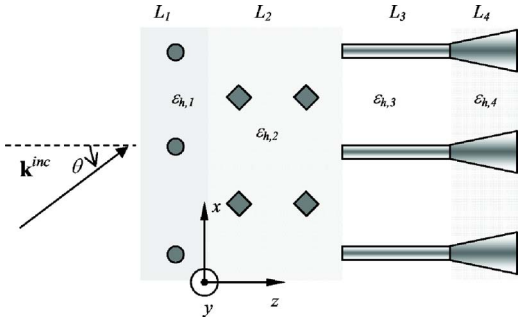

FIG. 3. (Color online) Geometry of a representative layered metamaterial. The structure has four layers, and each layer is associated with a different metamaterial slab. The salient elements (circles, squares, etc.) represent the dielectric inclusions. An incident wave with wave vector $\mathbf{k}^{\mathrm{inc}}$ illuminates the structure.

averaged over the directions of space along which the structure is periodic, but not along the z direction. In Ref. [8] a somehow related averaging concept was used to study impedance boundary conditions for thin material layers.

Later in the paper, we will explain how the TA fields can be used to characterize the scattering of waves by metamaterial slabs, knowing only the bulk medium effective parameters. Next, we will derive some completely general properties of the TA electric and induction fields.

To this end, we multiply both sides of the Maxwell equations by $\exp(j\mathbf{k}_\parallel \cdot \mathbf{r})$ and integrate the resulting expression over $\Omega_T(z)$ to obtain that

$$\left(-j\mathbf{k}_\parallel + \frac{\partial}{\partial z}\hat{\mathbf{u}}_z\right) \times \mathbf{E}_{\mathrm{av},T} = -j\omega \mathbf{B}_{\mathrm{av},T}$$

$$\left(-j\mathbf{k}_\parallel + \frac{\partial}{\partial z}\hat{\mathbf{u}}_z\right) \times \frac{\mathbf{B}_{\mathrm{av},T}}{\mu_0} = j\omega\varepsilon_h(z)\mathbf{E}_{\mathrm{av},T} + \mathbf{J}_{d,\mathrm{av}}(z), \quad (16)$$

where $\mathbf{J}_{d,\mathrm{av}}$ is the average polarization current relative to the host medium,

$$\mathbf{J}_{d,\mathrm{av}}(z) = \frac{1}{A_{\mathrm{cell}}} \int_{\Omega_T} \mathbf{J}_d(\mathbf{r}) e^{j\mathbf{k}_\parallel \cdot \mathbf{r}} dxdy, \quad (17)$$

and $\mathbf{J}_d = j\omega(\varepsilon - \varepsilon_h)\mathbf{E}$ is the polarization current. Note that if the permittivity of the structure is such that $\varepsilon(x,y,z) = \varepsilon(z)$, we can choose the permittivity of the host medium equal to $\varepsilon_h(z) = \varepsilon(z)$ and the polarization current vanishes. In these circumstances, the differential system (16) can be easily solved, and the TA fields calculated. However, in general, $\mathbf{J}_{d,\mathrm{av}}$ is unknown and its calculation may be as difficult as solving the original problem. This may suggest that the TA fields are difficult to obtain in a realistic problem. Ahead, we will prove that is not the case, and we will explain how the TA fields can be calculated for several geometries of interest provided the effective parameters of the associated bulk metamaterials are known. It is also important to underline that system (16) is exact and holds for a completely arbitrary structure periodic in the transverse plane. It is not by any means restricted to the case of planar grids parallel to the interfaces.

If the structure under study contains PEC inclusions, Eq. (17) becomes indeterminate (see the discussion of Sec. II A). The indetermination can be removed after straightforward calculations, but the details are omitted here. The result is

$$\mathbf{J}_{d,\mathrm{av}}(z) = \frac{1}{A_{\mathrm{cell}}} \left(\int_{\Omega_T - A_c(z)} \mathbf{J}_d e^{j\mathbf{k}_\parallel \cdot \mathbf{r}} dxdy + \int_{\partial A_c(z)} \mathbf{J}_c e^{j\mathbf{k}_\parallel \cdot \mathbf{r}} \frac{1}{|\hat{\nu} \times \hat{\mathbf{u}}_z|} dl \right), \quad (18)$$

where A_c is the intersection of the PEC metallic region (if any) with Ω_T (which depends on the z=const. plane; see Fig. 2), ∂A_c is the boundary of A_c, dl is the element of arc in ∂A_c, $\hat{\nu}$ is the outward unit vector normal to the metallic region, and $\mathbf{J}_c = \hat{\nu} \times \mathbf{B}/\mu_0$ is the density of current at the PEC inclusions. Note that $\mathbf{J}_{d,\mathrm{av}}$ is singular in the case of PEC planar inclusions normal to the z direction.

B. Boundary conditions for the transverse averaged fields

Next, we discuss the boundary conditions satisfied by the transverse averaged fields. Consider the geometry depicted in Fig. 3, which illustrates a representative layered artificial material structure. The structure is periodic in z=const. planes. The permittivity of the host medium in the ith layer is $\varepsilon_{h,i}$.

For simplicity, we will focus our attention in the case where the geometry of the structure is such that the tangential components of the microscopic fields $(\mathbf{E},\mathbf{B})$ are continuous at the pertinent z=const. plane (except possibly, over a set with zero measure). For most cases with practical interest this condition is satisfied. For example, for the structure shown in Fig. 3 the condition is satisfied at every z=const. plane in case of homogeneous dielectric inclusions. An example of a situation in which the transverse averaged fields are not continuous is the case of an array of PEC planar inclusions parallel to the interface. For that geometry, the tangential induction field is obviously discontinuous at the PEC inclusions plane because of the induced surface current.

When the tangential microscopic fields are continuous at some z=const. plane, it is obvious that the tangential TA fields, defined by Eq. (15), are also continuous at the same plane.

Let us study the continuity of the normal components (along z) of the TA fields. From Eq. (16) it is evident that the z component of the vectors in the left-hand side of both identities are continuous when the tangential TA fields are continuous. Therefore, we find that the vectors in the right-hand side have the same property, i.e.,

$$\hat{\mathbf{u}}_z \cdot [\mathbf{B}_{\mathrm{av},T}(z)] = 0, \quad (19)$$

$$\hat{\mathbf{u}}_z \cdot \left[\varepsilon_h(z)\mathbf{E}_{\mathrm{av},T} + \frac{\mathbf{J}_{d,\mathrm{av}}(z)}{j\omega} \right] = 0, \quad (20)$$

where the rectangular brackets represent the jump discontinuity of the vector inside the brackets at the considered plane, i.e., the vector evaluated at z^+ subtracted from the vector evaluated at z^-.

Equation (19) establishes that the normal component of the induction field is always continuous. This was expected because we admit from the beginning that the permeability of all components is μ_0, i.e., there are no magnetic inclusions (magnetic effects—if they exist—arise due to the circulation of electric currents).

On the other hand, Eq. (20) shows that the normal component of $\mathbf{E}_{\mathrm{av},T}$ is, in general, discontinuous. Let us study with more detail some special cases with practical interest. First let us consider that the inclusions do not intersect the z=const. plane of interest (for example, the interface $L1$-$L2$ in Fig. 3). In that case $\mathbf{J}_{d,\mathrm{av}}$ necessarily vanishes at that plane, and consequently,

$$\hat{\mathbf{u}}_z \cdot [\varepsilon_h(z)\mathbf{E}_{\mathrm{av},T}] = 0. \quad (21)$$

In particular, if the host medium is the same at both sides of the interface, $\mathbf{E}_{\mathrm{av},T}$ is a continuous vector.

Let us also analyze another important configuration. Consider the case in which the intersection of the inclusions with

the pertinent z=const. plane is a contour (a curve). This can only be relevant if the inclusions are PEC and hollow (e.g., if the inclusions are hollow PEC wires normal to the interface; this could correspond to section $L3$ in Fig. 3). If the PEC inclusions are broken at the plane of interest (e.g., interface $L2$-$L3$ in Fig. 3) the current that flows on their surface along the z direction must vanish, i.e., $\hat{\mathbf{u}}_z \cdot \mathbf{J}_{d,\mathrm{av}}=0$ (assuming that the adjacent material is nonconductive). But this result implies that at that plane, Eq. (21) also holds (even though the intersection of the inclusions with the plane is nontrivial). As proved in Ref. [19], in such circumstances, Eq. (21) can be regarded as an additional boundary condition, because it does not directly follow from the continuity of the tangential electromagnetic fields. This will be discussed with more detail later in the paper. Note that even though the enunciated result is (rigorously) valid only for hollow PEC inclusions, Eq. (21) also holds to a very good approximation when the PEC inclusions are not hollow but have a very small cross section.

Let us summarize our findings. We showed that except on some very special configurations, the tangential components of $(\mathbf{E}_{\mathrm{av},T}, \mathbf{B}_{\mathrm{av},T})$ are continuous at z=const. planes. We proved that in these circumstances $\mathbf{B}_{\mathrm{av},T}$ is necessarily a continuous vector, while the z component of $\mathbf{E}_{\mathrm{av},T}$ is in general, discontinuous. The derived results are understandable and intuitively correct, given the definitions of the TA fields [Eq. (15)].

However, at the same time, it is a bit puzzling that the boundary conditions satisfied by $(\mathbf{E}_{\mathrm{av},T}, \mathbf{B}_{\mathrm{av},T})$ have nothing to do with the classical boundary conditions in homogenized media. For example, the classical boundary conditions impose that the tangential component of the magnetic field $\mathbf{H}_{\mathrm{av}}=\frac{\mathbf{B}_{\mathrm{av}}}{\mu_0}-\mathbf{M}$ is continuous, rather than the tangential component of the induction field. Note that provided the magnetization vector $\mathbf{M}$ is different from zero, the two conditions are incompatible.

This important remark anticipates that, in general, the bulk medium fields (microscopic fields averaged over a unit cell) $\mathbf{E}_{\mathrm{av}}$ and $\mathbf{H}_{\mathrm{av}}$ are very different for the TA fields $\mathbf{E}_{\mathrm{av},T}$ and $\mathbf{B}_{\mathrm{av},T}$ (microscopic fields averaged over a cross section of the unit cell). In Sec. V, a formal relation between the bulk medium fields and the TA fields will be derived. It will be clearly explained why these fields satisfy completely different boundary conditions, and why these boundary conditions yield compatible results in the quasistatic limit.

C. Solution of the scattering problem using the transverse averaged-field approach

At this point it is important to explain how the formalism developed in the previous sections can be used in practice to solve a specific problem. The basic idea is illustrated in Fig. 1(b). As in the classical approach (Sec. II B), we assume that the low-frequency electromagnetic modes of the unbounded electromagnetic crystal are sufficient to characterize the fields inside the metamaterial slab, i.e., the effect of higher-order Floquet modes that cannot be modeled using homogenization theory is neglected.

The important difference as compared to the classical approach is that in our method the fields inside the slab are assumed to be a superimposition of the TA electromagnetic modes, instead of a superimposition of cell-averaged electromagnetic modes. In this way, the important variations of the fields along the z direction are not lost and are properly taken into account by the method. From the previous section, we have learned that the correct boundary conditions at the interfaces are the continuity of the tangential components of the TA electric and induction fields. Note that even though the TA fields have the Floquet property (with the same wave vector as the fields $\mathbf{E}_{\mathrm{av}}$ and $\mathbf{H}_{\mathrm{av}}$), their amplitude is not uniform along z. In particular, the polarization properties of the transverse averaged fields may vary with z.

Thus, the TA-field method proposed in this work can be summarized as follows. (i) In each metamaterial slab the fields are written in terms of TA fundamental electromagnetic modes of the associated unbounded electromagnetic crystal. (ii) At the interfaces the continuity of the tangential TA electric and induction fields is enforced.

It is clear that the scattering problem can be easily solved using the proposed recipe, provided the TA fields for the infinite lattice are known or can be computed. Quite interestingly, it turns out that for an important class of geometries it is immediate to relate the TA fields and the fields in the bulk medium. Or in other words, for some structures if we know the effective parameters of the unbounded electromagnetic crystal it is straightforward to compute the corresponding TA fields. This matter is discussed in the next section.

IV. TRANSVERSE AVERAGED FIELDS IN AN ELECTROMAGNETIC CRYSTAL

Here, we study the problem of calculation of TA fields in 3D-periodic electromagnetic crystals. As explained in Sec. III C, this matter is of crucial importance because to solve the scattering problem (Fig. 1) we assume that the fields inside each metamaterial slab can be written in terms of the (fundamental) transverse averaged Floquet modes of the infinite lattice.

The main result of this section establishes that when the metallic or dielectric inclusions are nearly planar, it is very simple to relate the TA fields with the macroscopic fields and the dielectric function of the metamaterial. In Sec. VI, we will prove that this result can be generalized for other geometries with nonplanar inclusions.

In what follows, it is assumed that the 3D-unbounded electromagnetic crystal has the same generic geometry as in Sec. II A. We suppose that the transverse plane is defined by the primitive vectors $\mathbf{a}_1$ and $\mathbf{a}_2$.

A. Integral representation of the transverse averaged fields

Next, we obtain an integral representation for the TA electric field associated with an arbitrary Floquet mode of the 3D-periodic lattice. For convenience, the wave vector of the considered Floquet mode is decomposed into a transverse and a longitudinal component: $\mathbf{k}=\mathbf{k}_{\|}+k_z\hat{\mathbf{u}}_z$.

To keep the readability of the paper, the detailed calculations have been moved to Appendix A. The results of the

Appendix A show that the TA electric field can be written exclusively in terms of the average polarization current $\mathbf{J}_{d,\mathrm{av}}$ associated with the Floquet mode, defined as in Eq. (17). The corresponding integral representation is

$$\mathbf{E}_{\mathrm{av},T}(z) = -j\omega\mu_0 A_{\mathrm{cell}} \int_{-a_\perp/2}^{a_\perp/2} \overline{\overline{\mathbf{G}}}_{0,T}(z|z') \cdot \mathbf{J}_{d,\mathrm{av}}(z')dz', \tag{22}$$

where we put $a_\perp = \mathbf{a}_3 \cdot \hat{\mathbf{u}}_z$ ($a_\perp > 0$). The dyadic $\overline{\overline{\mathbf{G}}}_{0,T}$ is defined by

$$\overline{\overline{\mathbf{G}}}_{0,T}(z|z';\mathbf{k}) = \left[\bar{\bar{\mathbf{I}}} + \frac{1}{\beta^2}\left(-j\mathbf{k}_\parallel + \frac{d}{dz}\hat{\mathbf{u}}_z\right)\left(-j\mathbf{k}_\parallel + \frac{d}{dz}\hat{\mathbf{u}}_z\right)\right] \times A_0(z-z';k_z), \tag{23}$$

where $\bar{\bar{\mathbf{I}}}$ is the identity dyadic, $\beta = \omega\sqrt{\varepsilon_h\mu_0}$ is the wave number in the host medium, and A_0 is the pseudoperiodic function of z (with wave number k_z) given by

$$A_0(z;k_z) = \frac{1}{2A_{\mathrm{cell}}\gamma_0}\left(e^{-\gamma_0|z|} + \sum_{\pm} \frac{e^{\pm\gamma_0 z}}{e^{a_\perp(\gamma_0 \pm jk_z)} - 1}\right). \tag{24}$$

In the above, $\gamma_0 = \sqrt{\mathbf{k}_\parallel \cdot \mathbf{k}_\parallel - \beta^2}$, and the sum with index ± represents the sum of two terms, one with the "+" sign and the other with the "−" sign. The formula is valid for $|z| < a_\perp$, but the function can be periodically extended to the whole space [20]. The field $\mathbf{B}_{\mathrm{av},T}$ is easily obtained from $\mathbf{E}_{\mathrm{av},T}$ using Eq. (16).

B. Relation between the transverse averaged fields and the bulk medium fields for nearly planar inclusions

Now that the necessary theoretical formalism has been introduced, we are ready to calculate the relation between $(\mathbf{E}_{\mathrm{av},T}, \mathbf{B}_{\mathrm{av},T})$ and $(\mathbf{E}_{\mathrm{av}}, \mathbf{B}_{\mathrm{av}})$ for a particular class of electromagnetic crystals. Let us suppose that the dielectric/metallic inclusions are relatively thin, so that to a first approximation it is possible to assume that they are contained in z=const. planes. Notice that this approximation applies to many metamaterials of interest, since as referred to before, the most common fabrication methods use planar technology. Furthermore, suppose that the inclusions in the unit cell are all contained in the same plane, $z=z_0$. In that case the average current $\mathbf{J}_{d,\mathrm{av}}$ vanishes everywhere in the unit cell except in the vicinity of the $z=z_0$ plane. Thus, within that approximation, the dyadic $\overline{\overline{\mathbf{G}}}_{0,T}$ can be moved outside of the integral in Eq. (22),

$$\mathbf{E}_{\mathrm{av},T}(z) = -j\omega\mu_0 A_{\mathrm{cell}} \overline{\overline{\mathbf{G}}}_{0,T}(z|z_0) \cdot \int_{-a_\perp/2}^{a_\perp/2} \mathbf{J}_{d,\mathrm{av}}(z')dz'. \tag{25}$$

It is simple to verify that the generalized polarization vector given by Eq. (6) can be rewritten as

$$\mathbf{P}_g = \frac{1}{j\omega a_\perp} \int_{-a_\perp/2}^{a_\perp/2} \mathbf{J}_{d,\mathrm{av}}(z) e^{+jk_z z} dz. \tag{26}$$

Substituting Eqs. (26) and (12) into Eq. (25), we readily find that

$$\mathbf{E}_{\mathrm{av},T}(z) = \mathrm{V}_{\mathrm{cell}} \beta^2 e^{-jk_z z_0} \overline{\overline{\mathbf{G}}}_{0,T}(z|z_0;\mathbf{k}) \cdot \left(\frac{\bar{\bar{\varepsilon}}_{\mathrm{eff}}}{\varepsilon_h} - \bar{\bar{\mathbf{I}}}\right) \cdot \mathbf{E}_{\mathrm{av}}. \tag{27}$$

This result establishes the desired relation between the TA electric field and the corresponding macroscopic electric field for a generic mode of the infinite lattice. It can be regarded as a generalization of the results derived in Ref. [14]. It shows that $\mathbf{E}_{\mathrm{av},T}$ can be written in terms of $\mathbf{E}_{\mathrm{av}}$, $\mathbf{k}$, and of the dielectric function $\bar{\bar{\varepsilon}}_{\mathrm{eff}}(\omega,\mathbf{k})$ of the bulk medium (see Sec. II A). Remember that for local media the dielectric function is expressed in terms of the permittivity and permeability tensors of the metamaterial, as shown in Eq. (13). We point out that Eq. (27) is not restricted to media with wire-dipole inclusions and can also be applied when the microscopic eddy currents are nontrivial. The TA induction field $\mathbf{B}_{\mathrm{av},T}$ can be obtained from $\mathbf{E}_{\mathrm{av},T}$ using Eq. (16).

Equation (27) shows that the TA fields can be readily computed if the bulk medium fields are known. This important result demonstrates that for the important class of nearly planar geometries we only need to know the dielectric function of the infinite lattice in order to apply the TA-field method.

C. Decomposition into transverse-electric and transverse-magnetic modes

As in the previous section, here we assume that the metallic or dielectric inclusions are nearly planar. In addition we suppose that the geometry of the inclusions and unit cell of the infinite crystal is such that the bulk medium average fields can be decomposed into two sets of modes (TE and TM), as explained next.

First, let us suppose that the dielectric function $\bar{\bar{\varepsilon}}_{\mathrm{eff}}$ of the periodic crystal is such that $\bar{\bar{\mathbf{I}}}_\parallel \cdot \mathbf{E}_{\mathrm{av}}$ satisfies

$$\left(\frac{\bar{\bar{\varepsilon}}_{\mathrm{eff}}}{\varepsilon_h} - \bar{\bar{\mathbf{I}}}\right) \cdot \bar{\bar{\mathbf{I}}}_\parallel \cdot \mathbf{E}_{\mathrm{av}} = (\varepsilon_{r,\parallel} - 1)\bar{\bar{\mathbf{I}}}_\parallel \cdot \mathbf{E}_{\mathrm{av}}. \tag{28}$$

In the above, $\bar{\bar{\mathbf{I}}}_\parallel = \hat{\mathbf{u}}_x\hat{\mathbf{u}}_x + \hat{\mathbf{u}}_y\hat{\mathbf{u}}_y$ and $\varepsilon_{r,\parallel}$ is the (transverse) relative permittivity seen by the electromagnetic mode.

As before, we write the wave vector of the electromagnetic modes as $\mathbf{k} = \mathbf{k}_\parallel + k_z\hat{\mathbf{u}}_z$. By definition, the set of TE modes (transverse electric to z) is formed by the electromagnetic modes with polarization such that

$$\mathbf{E}_{\mathrm{av}} \propto \hat{\mathbf{u}}_z \times \mathbf{k}_\parallel \quad \text{(TE modes)}. \tag{29}$$

On the other hand, the set of TM modes (transverse magnetic to z) is formed by the electromagnetic modes with polarization such that

$$\hat{\mathbf{u}}_z \times \mathbf{E}_{\mathrm{av}} \propto \hat{\mathbf{u}}_z \times \mathbf{k}_\parallel \quad \text{(TM modes)}. \tag{30}$$

If the dielectric function of the homogenized crystal is such that Eq. (28) holds, and if in addition the modes can be

decomposed into TE and TM modes, it can be easily proved that the corresponding TA fields given by Eq. (27) have the properties enunciated next.

First, the TA fields can also be decomposed into TE and TM modes. More specifically, the polarization of the TA fields is the same as the polarization of the bulk medium fields. Consequently, it makes sense to define a transverse impedance through the formula $\bar{Z}=\frac{\mu_0 E_{\mathrm{av},T,\|}}{B_{\mathrm{av},T,\|}}$. It can be readily verified that the transverse impedance is given by

$$\bar{Z}_{\mathrm{TE}}=\frac{-j\omega\mu_0 A_0}{\frac{dA_0}{dz}}, \tag{31}$$

$$\bar{Z}_{\mathrm{TM}}=\frac{-j\omega\mu_0 A_0}{\frac{dA_0}{dz}}\left(1-\frac{k_\|^2}{\beta^2}\right), \tag{32}$$

where A_0 is given by Eq. (24). Note that the transverse impedances defined above depend not only on frequency (β) and wave vector ($\mathbf{k}$), but also on the position z. Actually, since A_0 has the Floquet property, it is clear that the impedances $\bar{Z}_{\mathrm{TE}}$ and $\bar{Z}_{\mathrm{TM}}$ are periodic functions of coordinate z (with period $a_\perp$). But this is a very peculiar property. Indeed, while the impedances seen by the bulk medium modal fields ($\mathbf{E}_{\mathrm{av}},\mathbf{B}_{\mathrm{av}}$) are uniform and independent of z, quite differently, the impedances seen by the TA fields may vary strongly with z. This is a manifestation of the actual granularity and discreteness of the periodic structure.

Another very peculiar property is that the transverse impedance seen by a wave that propagates along the positive z direction is, in general, different from the impedance seen by the mode that propagates in the opposite direction: $\bar{Z}(z;k_z)\neq-\bar{Z}(z;-k_z)$. Note that in the bulk medium the transverse impedances are

$$\bar{Z}_{\mathrm{TE},b}=\frac{\omega\mu_0}{k_z}, \tag{33}$$

$$\bar{Z}_{\mathrm{TM},b}=\frac{\omega\mu_0}{k_z}\left(1-\frac{k_\|^2}{\beta^2}\right), \tag{34}$$

and so the relation $\bar{Z}_b(k_z)=-\bar{Z}_b(-k_z)$ is valid.

Even though, in general, the impedances seen by waves are different, there are specific planes of the crystal where the relation $\bar{Z}(k_z)=-\bar{Z}(-k_z)$ also holds. In fact, straightforward calculations show that

$$\bar{Z}(z_n;k_z)=-\bar{Z}(z_n;-k_z), \tag{35}$$

where $z_n=z_0+(\frac{1}{2}+n)a_\perp$ and n is an integer (remember that z_0 is the plane of the inclusions in the unit cell). This means that two waves that propagate in opposite directions see the same impedance only at planes spaced a half-lattice constant away from the inclusions. This result is very important because it shows that the effective interface between a metamaterial layer and (for example) free space is a half-lattice constant away from the inclusions at the boundary.

To conclude this section, we calculate the scattering parameters when a plane wave illuminates a metamaterial slab, as illustrated in Fig. 1. We suppose that the metamaterial is formed by N_L stacked layers, and that the interfaces with free space are chosen to be at planes of the form $z_n=z_0+(\frac{1}{2}+n)a_\perp$, so that the impedance seen by waves that propagate in opposite directions is the same. The thickness of the metamaterial slab is $L=N_L a_\perp$.

Let us suppose that the incoming plane wave is TE polarized, and that the incident wave vector is $\mathbf{k}=\mathbf{k}_\|+k_z^{\mathrm{inc}}\hat{\mathbf{u}}_z$, where $k_\|=\omega/c\cos\theta$ depends on the angle of incidence and $k_z^{\mathrm{inc}}=-j\sqrt{k_\|^2-\omega^2\varepsilon_0\mu_0}$, as explained in Sec. II B. The incident wave will excite only the TE mode inside the metamaterial slab. By ensuring the continuity of the tangential TA fields at the interface we easily find that the reflection coefficient (ratio between the reflected and incident electric fields) is

$$\rho_{\mathrm{TE}}=\frac{(\bar{Z}_{\mathrm{TE}}^2-\bar{Z}_0^2)j\tan(k_zL)}{2\bar{Z}_{\mathrm{TE}}\bar{Z}_0+(\bar{Z}_{\mathrm{TE}}^2+\bar{Z}_0^2)j\tan(k_zL)}, \tag{36}$$

where $\bar{Z}_0=\omega\mu_0/k_z^{\mathrm{inc}}$ is the transverse impedance seen by the incoming wave. Incidentally, the reflection coefficient predicted by classical theory is also given by the above formula, except that $\bar{Z}_{\mathrm{TE}}$ must be replaced by $\bar{Z}_{\mathrm{TE},b}$. Also, we note that in Eq. (36) k_z is the propagation constant of the TE mode excited inside the metamaterial slab, which can be easily calculated if the effective parameters of the associated infinite lattice are known, i.e., k_z is a function of frequency of the angle of incidence, and of the effective parameters of the bulk medium. In Sec. VI several specific examples will be given.

Using duality, it can be readily shown that the reflection coefficient for TM polarization (the ratio between the reflected and incident magnetic fields) is

$$\rho_{\mathrm{TM}}=\frac{(\bar{Y}_{\mathrm{TM}}^2-\bar{Y}_0^2)j\tan(k_zL)}{2\bar{Y}_{\mathrm{TM}}\bar{Y}_0+(\bar{Y}_{\mathrm{TM}}^2+\bar{Y}_0^2)j\tan(k_zL)}, \tag{37}$$

where $\bar{Y}_{\mathrm{TM}}=1/\bar{Z}_{\mathrm{TM}}$, $\bar{Y}_0=\omega\varepsilon_0/k_z^{\mathrm{inc}}$, and k_z is now the longitudinal propagation constant for TM modes. Similar formulas can be derived for the transmission coefficients.

V. RELATION BETWEEN THE TRANSVERSE AVERAGED FIELDS AND THE MACROSCOPIC FIELDS FOR VERY LONG WAVELENGTHS

It is conceptually clear that the TA fields ($\mathbf{E}_{\mathrm{av},T},\mathbf{B}_{\mathrm{av},T}$) may be more effective than the bulk medium fields ($\mathbf{E}_{\mathrm{av}},\mathbf{B}_{\mathrm{av}}$) in the characterization of an artificial material slab. However, in classical works, and, in particular, in the study of the propagation of radiation in matter, the bulk medium fields are invariably used. It is thus important to understand why and when such a theory may, in fact, be so successful. In this section, we make the connection between the two approaches.

We investigate the properties of the transverse averaged modal fields in the long wavelength limit regime: $|\gamma_0 a_\perp|\ll\pi$ and $|k_z a_\perp|\ll\pi$. The details of the calculations are pre-

sented in Appendix B. It is proved that if the induced microscopic currents can only excite electric and/or magnetic dipole moments, the following formulas hold at z=const. planes that do not intersect the inclusions:

$$\mathbf{E}_{\mathrm{av},T} \approx \mathbf{E}_{\mathrm{av}} + \hat{\mathbf{u}}_z \hat{\mathbf{u}}_z \cdot \frac{\mathbf{P}}{\varepsilon_h}, \tag{38}$$

$$\frac{\mathbf{B}_{\mathrm{av},T}}{\mu_0} \approx \frac{\mathbf{B}_{\mathrm{av}}}{\mu_0} + \hat{\mathbf{u}}_z \times (\hat{\mathbf{u}}_z \times \mathbf{M}), \tag{39}$$

where $\mathbf{P}$ and $\mathbf{M}$ are the polarization and magnetization vectors, respectively [see Eqs. (9) and (10)]. The above formulas clearly explain why the boundary conditions verified by the TA fields are compatible with the classical boundary conditions, and, consequently, prove that for very long wavelengths the TA-field approach is equivalent to the classical approach.

Indeed, as discussed in Sec. III B, the tangential components of both the TA electric and induction fields are continuous at an interface. But, this property together with Eqs. (38) and (39) imply that the tangential components of $\mathbf{E}_{\mathrm{av}}$ and $\mathbf{H}_{\mathrm{av}} = \frac{\mathbf{B}_{\mathrm{av}}}{\mu_0} - \mathbf{M}$ are continuous. But these are precisely the classical boundary conditions.

Similarly, consistently with classical theory, Eqs. (19) and (39) demonstrate that the normal component of $\mathbf{B}_{\mathrm{av}}$ is continuous at an interface, and Eqs. (21) and (38) confirm that the normal component of the electric displacement vector $\mathbf{D}_{\mathrm{av}} = \varepsilon_h \mathbf{E}_{\mathrm{av}} + \mathbf{P}$ is continuous as well.

VI. APPLICATION OF THE METHOD AND DISCUSSION

Here, we will apply the TA-field method to several relevant metamaterial geometries, and compare the obtained results with classical reflection theory and with full wave numerical simulations obtained with an electromagnetic simulator based on the method of moments (MoM) [21].

A. ε-Negative dielectric rods

In the first example, we investigate the reflection of waves by a screen of ENG rods. This artificial material recently aroused a great interest because it may play a very important role in subwavelength imaging applications at infrared and optical frequencies [6,22,23], using the canalization mechanism proposed in Ref. [24]. The ENG rod medium is formed by a square lattice of infinitely long metallic rods with radius R [23]. At the infrared and optical frequencies all metallic materials lose their conducting properties, and to a good approximation their permittivity follows the Drude model. In particular, the real part of the permittivity is negative.

We will suppose that the rods are oriented along the y direction, as illustrated in the inset of Fig. 4. The relative permittivity of the rods is $\varepsilon_{\mathrm{rod}}$ and the volume fraction of the rods is $f_V = \pi(R/a)^2$. In Ref. [23] we proved that the ENG-rod medium can be modeled by an effective permittivity such that $\varepsilon_{xx} = \varepsilon_{zz} \approx 1$, and

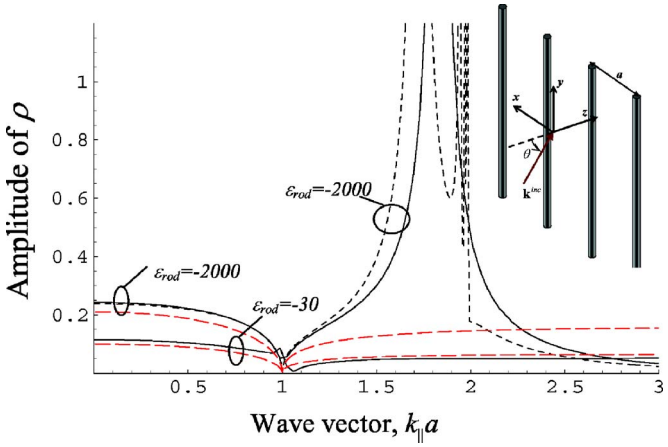

FIG. 4. (Color online) Amplitude of the reflection coefficient as a function of $k_\|$ for different permittivities of the ENG dielectric rods. The incident wave is TM-z polarized. The normalized frequency is $\beta a = 1.0$. Solid (black) line: full wave results; Dashed (black) line: TA-field method; Short-dashed (red - light gray in grayscale) line: classical theory. The inset shows the geometry of the ENG rods.

$$\varepsilon_{yy} = 1 + \frac{1}{\dfrac{1}{(\varepsilon_{\mathrm{rod}} - 1) f_V} - \dfrac{\beta^2 - k_y^2}{\beta_p^2}}, \tag{40}$$

where β_p is the plasma wave number, which depends on the radius of the wires and lattice constant. Because of the spatial dispersion effects, the effective permittivity of the rods is a function of both frequency $\beta = \omega/c$ and wave vector k_y. For further details the reader is referred to our previous publication.

Here, the objective is to study the reflection from a (quasiplanar) screen of ENG rods (the slab with one layer). We suppose that the rods are embedded in air and are positioned at $(na, 0, 0)$, with n integer. Based on the results of Sec. IV, we consider that the interfaces of the equivalent metamaterial slab are $(0, 0, -a/2)$ and $(0, 0, a/2)$. The incident plane wave is TM-z polarized (the magnetic field is along the x direction). The transverse component of the wave vector is $\mathbf{k}_\| = (0, k_y, 0)$. The angle of incidence satisfies $\sin\theta = k_y/\beta$. Using the permittivity model (40), it can be verified that for this specific configuration the incident wave only excites one electromagnetic mode in the ENG-rod medium. The longitudinal propagation constant k_z satisfies

$$k_z^2 = -k_x^2 + (\beta^2 - k_y^2)\varepsilon_{yy}. \tag{41}$$

Even though in the general case the waves in the metamaterial cannot be decomposed into TE and TM waves relative to the z direction, such decomposition is possible for the $k_x = 0$ case, and so we can use the very convenient closed-form formula (37) to obtain the reflection coefficient at the interface. As explained in Sec. IV, the formula is valid for both the TA-field approach and classical theory, with the difference that the transverse impedances are different.

In Fig. 4 we plot the amplitude of the reflection coefficient as a function of $k_{\|}a$ (i.e., as a function of the angle of incidence) at the fixed normalized frequency $\beta a=1.0$. Two cases are plotted: (i) $\varepsilon=-30$ and $R=0.05a$ (which corresponds to $\beta_p a=1.88$) and (ii) $\varepsilon=-2000$ and $R=0.01a$ (which corresponds to $\beta_p a=1.37$). The solid line corresponds to the full wave results, the dashed black line to the TA-field method, and the short-dashed red (light gray in grayscale) line to classical theory. We point out that the full wave results can be regarded as the exact solution of the problem, apart from small unavoidable numerical errors intrinsic to the method of moments. We also note that for $k_{\|}>\beta$ the incident wave is an evanescent decaying mode, and consequently, the reflection coefficient can be greater than unity without violating energy conservation. It is seen that for propagating waves the results of our method are practically coincident with full wave simulations; the results of classical theory—even though not so accurate—also follow reasonably well the full wave results.

From Fig. 4 it is seen that for $\varepsilon_{\mathrm{rod}}=-2000$ the reflection coefficient has a pole around $k_y a=1.8$ (evanescent wave spectrum). This means the ENG rod screen supports a surface wave mode that propagates tightly attached to the rods and decays exponentially away from the rods. It is seen in Fig. 4 that our approach nicely predicts this effect (apart from some ripple at the resonance), while the classical method fails to predict the result. The observed ripple at the resonance is also characteristic of other examples studied ahead. Apparently, the reason is that the homogenization model fails to some extent near resonance, which is understandable from a physical point of view. This surface wave mode can be used to guide a wave along the rods and eventually achieve subdiffraction propagation, but such a discussion is outside the scope of this paper. A similar agreement is obtained for the phase of the reflection coefficient and for the transmission coefficient.

B. Connected perfectly electric conducting wires parallel to the interface

Next, we will study the reflection properties of slabs formed by layers of connected PEC wires parallel to the interface (the 2D mesh of connected wires, also known as 2D-wire medium). This problem is relevant on its own because metal meshes, perforated plates, and wire grids are widely used as elements of quasioptical devices such as polarizing filters, quasioptical gratings, and semitransparent mirrors. Also these meshes can be used to fabricate artificial ENG media, and may play an important role in different problems [1].

The geometry of the wire mesh is illustrated in the inset of Fig. 5. The wires are oriented along the x and y directions. The spacing between parallel wires is a. Notice that the wires are connected at the intersection points. The infinite lattice (periodic crystal) consists of an array of screens similar to the one depicted in the inset of Fig. 5. The spacing between the screens is also a. Recently [12], it was proved that this electromagnetic crystal can be characterized by the following permittivity model:

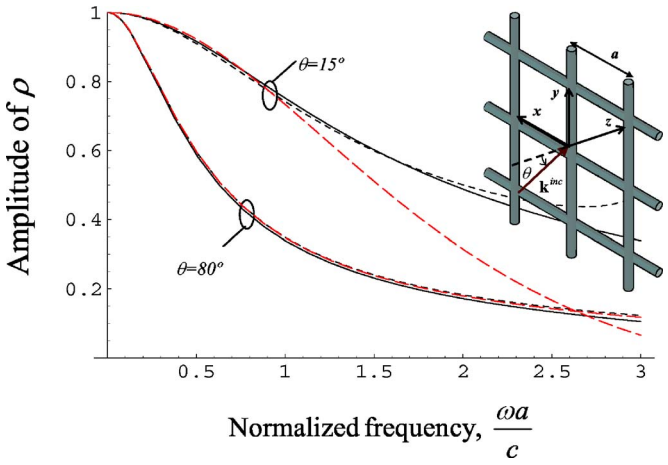

FIG. 5. (Color online) Amplitude of the reflection coefficient as a function of normalized frequency. The incident wave is TM polarized and propagates along the direction $(\phi=45,\theta)$ (deg). Solid (black) line: full wave results; dashed (black) line: TA-field method; short-dashed (red—light gray in grayscale) line: classical theory. The inset shows the geometry of the 2D-wire mesh.

$$\bar{\bar{\varepsilon}}=\bar{\bar{\mathbf{I}}}-\frac{\beta_p^2}{\beta^2}\left(\bar{\bar{\mathbf{I}}}_{\|}-\frac{\mathbf{k}_{\|}\mathbf{k}_{\|}}{k_{\|}^2-l_0\beta^2}\right),\quad l_0=\frac{2}{1+\dfrac{\beta_p^2}{\beta_1^2}}. \tag{42}$$

In the above formula, the symbols $\mathbf{k}_{\|}=(k_x,k_y,0)$ and $\bar{\bar{\mathbf{I}}}_{\|}=\hat{\mathbf{u}}_x\hat{\mathbf{u}}_x+\hat{\mathbf{u}}_y\hat{\mathbf{u}}_y$ are defined consistently with our previous notations, and β_p is the plasma wave number of the effective medium. The constant β_1 only depends on the lattice constant a and on the radius of the wires R, and can be calculated as explained in Ref. [12]. In all the examples we assume that the radius of the wires is $R=0.01a$, and so $\beta_p a=1.37$ and $\beta_1 a=3.55$. Notice also that as in the previous section the effective permittivity of the electromagnetic crystal depends on the wave vector as a manifestation of spatial dispersion (this phenomenon is characteristic of all wire-based metamaterials [12]).

Using Eq. (42), it can be easily verified that the modal solutions of the infinite lattice can be decomposed into TE and TM modes relative to the z direction. The dispersion characteristic of the TM and TE modes is given by

$$k_{z,\mathrm{TM}}^2=(\beta^2-k_{\|}^2)\varepsilon_{\mathrm{TM}}, \tag{43}$$

$$k_{z,\mathrm{TE}}^2=\beta^2\varepsilon_{\mathrm{TE}}-k_{\|}^2, \tag{44}$$

where $\varepsilon_{\mathrm{TE}}=1-\beta_p^2/\beta^2$ and $\varepsilon_{\mathrm{TM}}=1-\frac{\beta_p^2}{\beta^2}\left(1-\frac{k_{\|}^2}{k_{\|}^2-l_0\beta^2}\right)$ are the transverse permittivities seen by the TE and TM modes, respectively. Since the fields can be decomposed into TE and TM modes we can apply the results of Sec. IV, and in particular we can use Eqs. (36) and (37) to calculate the reflection characteristic. As in the previous section, the equivalent interfaces of the metamaterial slab are placed a half-lattice constant away from the wire mesh.

In the first example, we study the reflection properties as a function of normalized frequency and for different incident angles (Figs. 5 and 6). The angle of incidence is defined by

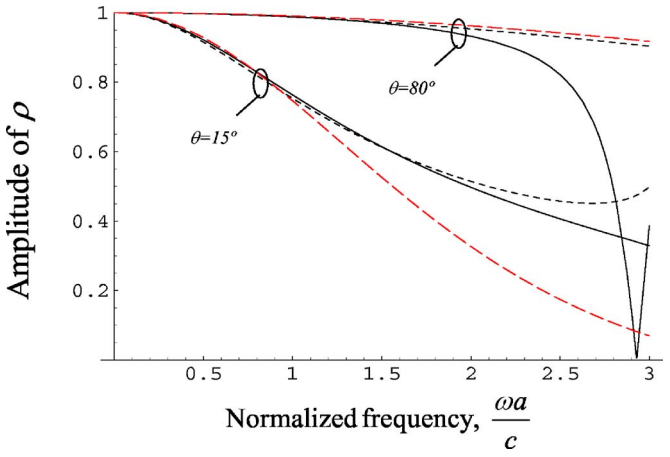

FIG. 6. (Color online) Amplitude of the reflection coefficient as a function of the normalized frequency. The incident wave is TE polarized and propagates along the direction $(\phi=45,\theta)$ (deg). The line styles are as in Fig. 5.

angle ϕ (measured relative to the x axis in the xoy plane) and angle θ (measured relative to the z axis). Thus, the transverse wave vector is $\mathbf{k}_{\parallel}=\beta(\cos\theta\cos\phi,\cos\theta\sin\phi,0)$. It is seen from the figures that our method agrees very well with full wave simulations for normalized frequencies as large as $\beta a=2.0$. Quite differently, the classical approach is only accurate for normalized frequencies such that $\beta a<1.0$ (the error is noticeable mainly for paraxial incidence).

In the second example, we investigate the effect of increasing the number of screens. In Fig. 7 the reflection coefficient is shown for TM polarization (the magnetic field is parallel to the screen) and $\theta=45$ (deg) and $N_L=1$, 2, and 3 layers. It is seen that the agreement between the classical approach and full wave simulations improves when the number of layers increases. On the other hand, the results predicted by our method are excellent, independent of the number of layers.

In the last example, we examine if the homogenization method can predict the reflection characteristic of evanescent

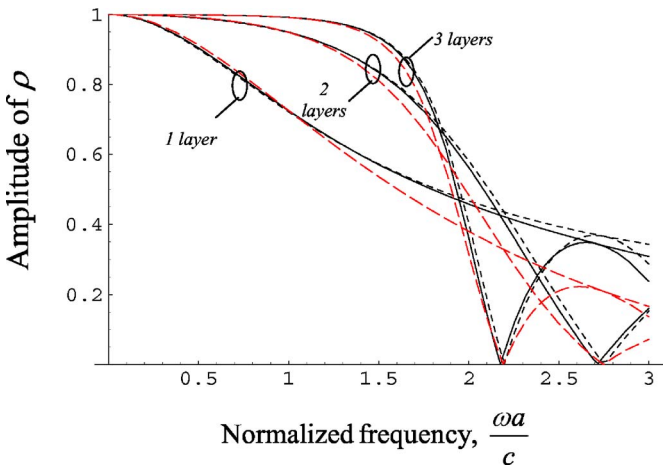

FIG. 7. (Color online) Amplitude of the reflection coefficient as a function of the normalized frequency for different slab thicknesses. The incident wave is TM polarized and propagates along the direction $(\phi=45,\theta=45)$ (deg). The line styles are as in Fig. 5.

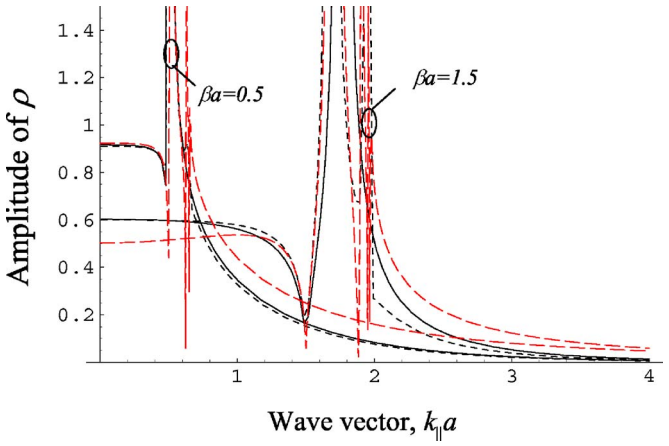

FIG. 8. (Color online) Amplitude of the reflection coefficient as a function of $k_{\parallel}$. The incoming wave is TM polarized. The line styles are as in Fig. 5.

modes. In Figs. 8 and 9 the amplitude of the reflection coefficient is shown as a function of $k_{\parallel}$ for the normalized frequencies $\beta a=0.5$ and $\beta a=1.5$, and propagation along $\phi=0$ (deg). The metamaterial slab has only one layer. It is verified that even though both homogenization methods follow reasonably well the full wave simulations, the TA-field technique is clearly more accurate. In Fig. 8 it is seen that for TM polarization the wire mesh supports a surface wave mode that propagates attached to the wires. Quite differently, for TE polarization (electric field is parallel to the screen) such a mode does not exist. We also point out that the classical permittivity model for the 2D-wire mesh (with no spatial dispersion and $\varepsilon_{\mathrm{TM}}=1-\beta_p^2/\beta^2$), completely fails to predict the dispersion characteristic of the evanescent modes (not shown here). This demonstrates that the permittivity model (42) is better than the classical model.

C. Crossed perfectly electric conducting wire mesh parallel to the interface

Now, we examine the properties of a configuration closely related to the screen of connected wires studied before: the

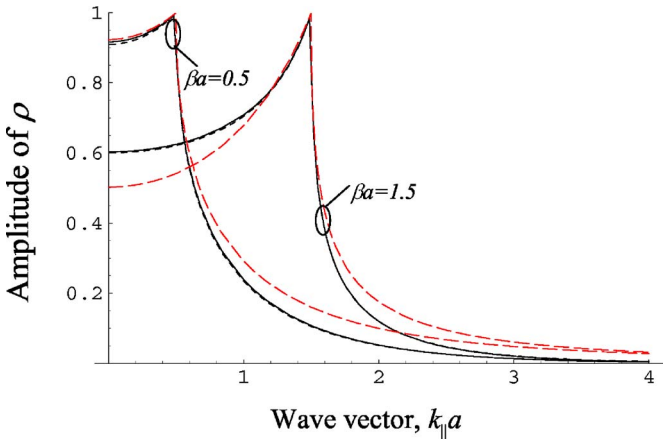

FIG. 9. (Color online) Amplitude of the reflection coefficient as a function of $k_{\parallel}$. The incoming wave is TE polarized. The line styles are as in Fig. 5.

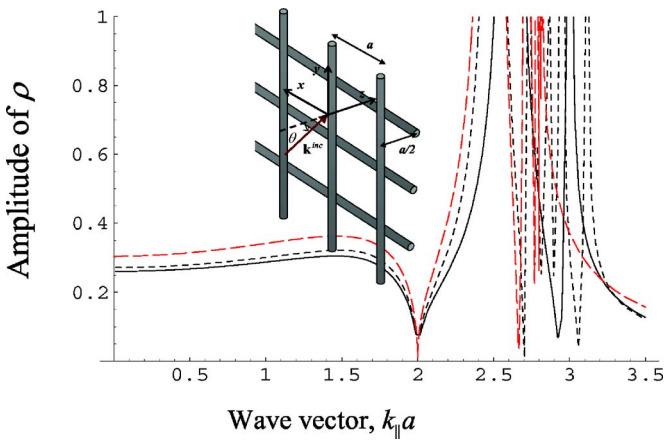

FIG. 10. (Color online) Amplitude of the reflection coefficient as a function of $k_\parallel$. The incident wave is TM polarized and propagates along $\phi=45$ (deg). The normalized frequency is $\beta a=2.0$. Solid (black) line: full wave results; dashed (black) line: TA-field method; short-dashed (red—light gray in grayscale) line: classical theory. The inset shows the geometry of the metamaterial slab (one layer).

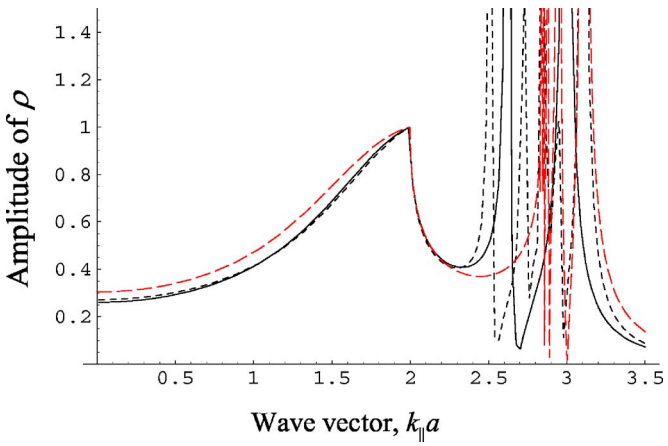

FIG. 11. (Color online) Amplitude of the reflection coefficient as a function of $k_\parallel$. The incident wave is TE polarized and propagates along $\phi=45$ (deg). The normalized frequency is $\beta a=2.0$. The line styles are as in Fig. 10.

metamaterial is formed by a crossed wire mesh of nonconnected wires. This problem was already investigated in our previous publication [14]. Here, we will look at the reflection characteristic of evanescent modes, which was not studied in Ref. [14].

As in the previous section, the PEC wires are oriented along the x and y directions, but now the wires are nonconnected: orthogonal wires are spaced by half-lattice constant, $a/2$. The geometry of the metamaterial slab (one layer) is depicted in the inset of Fig. 10. The periodic crystal is formed by juxtaposing metamaterial slabs with thickness a.

Note that for this periodic structure the inclusions in the unit cell are not contained in the same $z=$const. plane: in fact the wire along the x direction is near the plane $z=z_y\equiv -a/4$ and the wire along the y direction is near the plane $z=z_x\equiv +a/4$. Thus, Eq. (27), and in particular, the results of Sec. IV, are not valid. However, it was proved in Ref. [14] that the TA-electric field can still be related with the average field in the bulk crystal. The pertinent formula is (in our present notations)

$$\mathbf{E}_{\mathrm{av},T}(z) = V_{\mathrm{cell}}\beta^2 \sum_{i=x,y} e^{-jk_z z_i}\overline{\overline{\mathbf{G}}}_{0,T}(z|z_i;\mathbf{k})\cdot \hat{\mathbf{u}}_i\hat{\mathbf{u}}_i\cdot(\varepsilon_{ii}-1)\mathbf{E}_{\mathrm{av}}, \tag{45}$$

where ε_{ii} is the relative permittivity of the infinite lattice along the wires [12,14,25],

$$\varepsilon_{ii} = 1 - \frac{\beta_p^2}{\beta^2 - k_i^2}, \quad i=x,y. \tag{46}$$

Equation (45) can be easily derived using the same arguments as in Sec. IV C, noting that the average current $\mathbf{J}_{d,\mathrm{av}}$ vanishes everywhere in the unit cell except in the vicinity of the $z=z_x$ and $z=z_y$ planes, and that only the wires directed along the i direction ($i=x,y$) contribute to the effective permittivity along the same direction. The scattering problem is solved as delineated in Sec. III C. For further details the reader is referred to Ref. [14].

In Figs. 10 and 11 we depict the reflection characteristic of the wire mesh at the normalized frequency $\beta a=2.0$, and for TM- and TE-polarized incident waves propagating along $\phi=45$ (deg), respectively (the angle ϕ is defined as in the previous section; the radius of the rods is $R=0.01a$). It is seen that our method (dashed black line) compares well with the full wave results (solid line) apart from the ripple at the resonances. It is also observed that unlike in the case of connected wires, both polarizations can excite a surface wave mode that propagates tightly bounded to the metamaterial slab. Indeed, this is not really surprising because, as reported in Ref. [14], the cross-polarization level can be very high due to the fact of the wires not being connected. This is illustrated in Fig. 12. Notice that classical theory predicts that the cross-polarization level is zero in total disagreement with the full wave simulations [indeed for $\phi=45$ (deg), it is clear that $\varepsilon_{xx}=\varepsilon_{yy}$ and so the waves in the bulk medium can

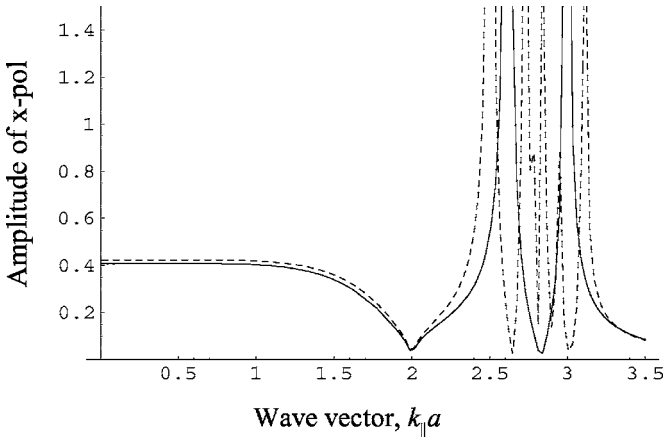

FIG. 12. Cross-polarization level as a function of $k_\parallel$. The incident wave propagates along $\phi=45$ (deg). The normalized frequency is $\beta a=2.0$. The line styles are as in Fig. 10. Notice that classical theory predicts that the x-pol level is zero.

be decomposed into TE and TM modes relative to z]. To conclude, we also refer that unlike in the case of connected wires, the full wave simulations show that the nonconnected wires support two different surface wave modes.

D. Perfectly electric conducting wires normal to the interfaces

In all the examples studied so far, the inclusions in the unit cell were nearly contained in $z=$const. planes. Nevertheless, our approach can also be readily applied to some configurations in which the inclusions are not quasiplanar. To demonstrate this, we will briefly discuss the scattering of waves by an array of PEC wires normal to the interface (i.e., the wires are directed along the z direction). The distance between the wires is a. It is worth noting that besides being theoretically interesting, this metamaterial setup has very important applications. In Ref. [6] and [22] it was demonstrated that at microwaves such a wire medium lens is able to transport the subwavelength details of an image to nearly unlimited distances. Moreover, the metamaterial can also be used to fabricate nearly ideal (for a specific polarization) artificial impedance surfaces, and in particular, artificial magnetic conductors [8] (Fakir's bed of nails configuration).

Since the wire inclusions are not contained in a $z=$const. plane, the results of Sec. IV do not apply. However, it is still simple to relate the TA field with the bulk medium field. To this end, we remember that the unbounded electromagnetic crystal is formed by infinitely long metallic wires oriented along the z direction. Thus, the electromagnetic modes in the PEC wire medium are such that $\mathbf{E}(x,y,z)=\mathbf{E}(x,y)e^{-jk_z z}$, and in particular, the average current is such that $\mathbf{J}_{d,\mathrm{av}}(z)=\mathbf{J}_{d,\mathrm{av}}e^{-jk_z z}$. Substituting this result in Eq. (22), and using Eq. (6) and the formula

$$\int_{-a_\perp/2}^{a_\perp/2} \bar{\bar{\mathbf{G}}}_{0,\mathcal{T}}(z|z';\mathbf{k})e^{-jk_z z'}dz' = \frac{1}{A_{\mathrm{cell}}\beta^2}\frac{\beta^2\bar{\bar{\mathbf{I}}}-\mathbf{kk}}{k^2-\beta^2}e^{-jk_z z}, \tag{47}$$

we find that

$$\mathbf{E}_{\mathrm{av},\mathcal{T}}(z) = \frac{\beta^2\bar{\bar{\mathbf{I}}}-\mathbf{kk}}{k^2-\beta^2}\cdot\frac{\mathbf{P}_g}{\varepsilon_h}e^{-jk_z z}. \tag{48}$$

Finally, using Eqs. (4) and (5) to simplify the right-hand side of the equation, we obtain that

$$\mathbf{E}_{\mathrm{av},\mathcal{T}}(z) = \mathbf{E}_{\mathrm{av}}e^{-jk_z z}. \tag{49}$$

Thus, we found that in an electromagnetic crystal of infinitely long PEC wires the TA electric field (relative to the z direction) is coincident with the bulk medium field. A similar relation holds for the magnetic field. At first sight this result may seem surprisingly simple, but indeed it is a trivial consequence of the fact that the dependence of the electromagnetic modes with z is of the form $e^{-jk_z z}$.

Thus, the previous result suggests that for this configuration the classical approach yields the same results as the transverse averaged-field method. In fact, things are not really so simple. The problem is that the wire medium is strongly spatially dispersive for long wavelengths, and as a consequence it supports three electromagnetic modes for low frequencies, instead of two electromagnetic modes as common materials. Due to this reason, the classical boundary conditions (continuity of the tangential components of the fields) are insufficient to solve the scattering problem. Recently, we proved that an additional boundary condition (ABC) is necessary to properly solve this problem [19]. Consistently, with the discussion of Sec. III B, the new ABC imposes that Eq. (21) holds, i.e., the normal component of the average electric field multiplied by the permittivity of the host medium is continuous at the interface. For more details the interested reader is referred to Refs. [19,22], where the homogenization of the metamaterial slab under study was extensively validated.

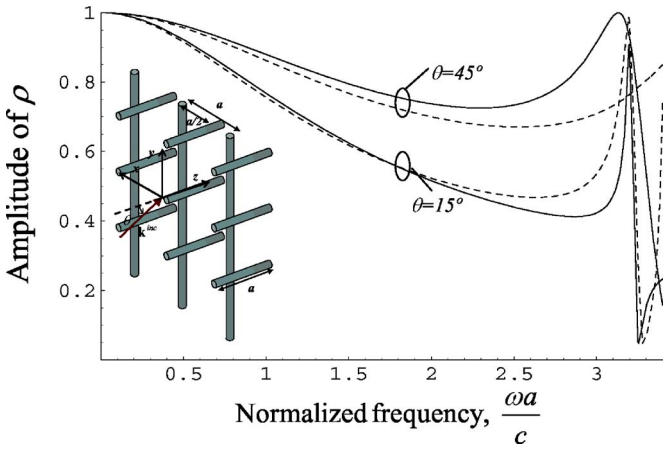

FIG. 13. (Color online) Amplitude of the reflection coefficient as a function of normalized frequency for different angles of incidence. The incident wave is TM polarized. Solid line: full wave results; dashed line: TA-field method. The inset shows the geometry of the crossed wire mesh (one-layer).

E. Crossed perfectly electric conducting wire mesh normal to the interface

The results of the previous section can be readily generalized to other metamaterial configurations with wires normal to the interface. To illustrate this, we consider (as in Sec. VI C) that the infinite lattice consists of a crossed wire mesh of nonconnected infinitely long wires. However, here we suppose that the wires are oriented along the y and z directions, so that the geometry of a metamaterial slab (one layer) is as shown in the inset of Fig. 13. The spacing between parallel wires is a, and the spacing between orthogonal wires is $a/2$.

To calculate the TA-modal fields in the infinite lattice we proceed as explained next. First of all, it is noted that the averaged current $\mathbf{J}_{d,\mathrm{av}}(z)$ only has components along y and z. The component along the y direction vanishes everywhere in the unit cell, except at the plane $z=z_y$ that contains the wires along the y direction. On the other hand, the component of $\mathbf{J}_{d,\mathrm{av}}(z)$ along z is different from zero for every z. Within the thin wire approximation, it is legitimate to suppose that the current along the z-directed wires is a traveling wave with propagation factor $e^{-jk_z z}$ [12]. Hence, we can assume that

$\hat{\mathbf{u}}_z \cdot \mathbf{J}_{d,\mathrm{av}}(z) \approx \hat{\mathbf{u}}_z \cdot \mathbf{J}_{d,\mathrm{av}} e^{-jk_z z}$ (note that this relation is the analog of the result used in Sec. VI D; here, unlike in Sec. VI D, the formula is only an approximation). Based on these considerations, and proceeding as in Secs. IV and VI D, it can be readily proved that the transverse averaged field of the electromagnetic modes is given by

$$\mathbf{E}_{\mathrm{av},T}(z) = \beta^2 V_{\mathrm{cell}} \bar{\bar{\mathbf{G}}}_{0,T}(z|z_y;\mathbf{k}) e^{-jk_z z_y} \cdot \hat{\mathbf{u}}_y \hat{\mathbf{u}}_y \cdot (\varepsilon_{yy} - 1)\mathbf{E}_{\mathrm{av}} + \frac{\beta^2 \bar{\bar{\mathbf{I}}} - \mathbf{kk}}{k^2 - \beta^2} e^{-jk_z z} \cdot \hat{\mathbf{u}}_z \hat{\mathbf{u}}_z \cdot (\varepsilon_{zz} - 1)\mathbf{E}_{\mathrm{av}}, \quad (50)$$

where $\mathbf{E}_{\mathrm{av}}$ is the average modal field in the infinite lattice and $\varepsilon_{ii} = 1 - \frac{\beta_p^2}{\beta^2 - k_i^2}$ $(i = y, z)$ are the components of the effective permittivity.

To solve the scattering problem, we still need to characterize the electromagnetic modes of the infinite lattice. For simplicity, we will assume propagation in the *yoz* plane, i.e., that $k_x = 0$. In that case, the waves in the bulk medium can be decomposed into TM and TE modes relative to the z direction. Using the effective permittivity model of the crossed wire mesh [12,14,25] it can be easily verified that the dispersion characteristic of the TM modes (magnetic field is directed along x) is

$$k_z^2 = \frac{1}{2}\left(Q \pm \sqrt{Q^2 + 4\beta^2 \varepsilon_{yy}(\beta_p^2 - \beta^2 + k_y^2)}\right),$$

$$Q = \beta^2 - \beta_p^2 + \varepsilon_{yy}(\beta^2 - k_y^2). \quad (51)$$

The polarization of the TM modes (assuming always that $k_x = 0$) is such that

$$\mathbf{E}_{\mathrm{av}} \propto (0, k_y k_z, k_z^2 - \beta^2 \varepsilon_{yy}). \quad (52)$$

As mentioned above, the average magnetic field is oriented along the x direction.

The reflection problem can now be solved by matching the TA fields [calculated using Eqs. (50) and (16)] at the interfaces, as explained in Sec. III C. We assume that the incident wave is TM-z polarized and propagates in the *yoz* plane; thus, only TM-z modes can be excited in the metamaterial slab [the dispersion characteristic of these modes is given by Eq. (51)]. However, there is still an additional difficulty. The problem is that Eq. (51) shows that the metamaterial slab supports two different TM modes (two different solutions for k_z^2) while the free-space region only supports one TM mode. Thus, it is clear that as in the previous section an ABC is necessary [19]. It was demonstrated in Sec. III B that because the current along the z-directed wires must vanish at the interfaces, this boundary condition is still given by (21). Hence to solve the scattering problem we need to impose not only the continuity of the tangential TA-electromagnetic fields, but also the ABC (21). It is important to refer that for long wavelengths the two TM modes supported by the metamaterial slab [given by Eq. (51)] have a longitudinal propagation constant of the form $jk_z = \alpha_z \pm j\beta_z$, where α_z and β_z are some constants that depend on the frequency and on the transverse wave vector. Hence, both modes are evanescent and have the same attenuation constant. Thus, it is not possible to neglect one of the modes and avoid the ABC.

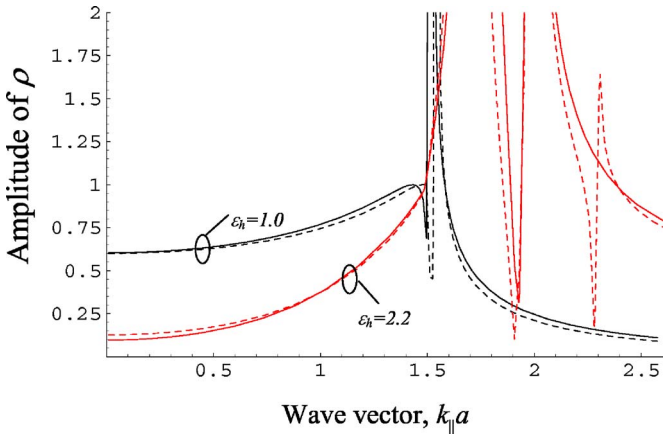

FIG. 14. (Color online) Amplitude of the reflection coefficient as a function of $k_\parallel$ for different permittivities of the host material. The incident wave is TM polarized. The normalized frequency is $\beta a = 1.5$. The line styles are the same as in Fig. 13.

In order to illustrate the application of the results we have computed the reflection characteristic of the metamaterial slab (one layer) as a function of normalized frequency and for different angles of incidence. The results are shown in Fig. 13, revealing a good agreement between our method and full wave simulations. We do not present results for classical theory since as discussed before, the ABC condition cannot be ignored (in fact, if the ABC condition was discarded and classical theory was applied, the results would be nonphysical with the amplitude of the reflection coefficient greater than unity). In Fig. 14 we plot the reflection characteristic for propagating and evanescent modes at the normalized frequency $\beta a = 1.5$. We assume that the wires are either embedded in air ($\varepsilon_h = 1$) or in a material with permittivity $\varepsilon_h = 2.2$. In both cases the agreement is good, and consistently with the full wave simulations, our theory predicts that the metamaterial slab supports a surface wave mode.

F. Metallic patches parallel to the interfaces

In this section, we will study the reflection of waves by a screen formed by metallic PEC patches parallel to the interfaces. The objective of the analysis is twofold. The first objective is to explain how the TA-field method can be applied when an analytical model for the effective permittivity of the infinite lattice is not readily available. Note that in all the examples studied before the effective parameters of the electromagnetic crystal were known in closed-analytical form. The second objective is to demonstrate that our method can also be applied when the infinite lattice has a nontrivial effective permeability.

The periodic medium is formed by a cubic array of metallic patches with lattice constant a. The structure can be seen as an array of aligned screens spaced by the distance a. The inset of Fig. 15 illustrates the geometry of one layer of the periodic material. The patches are planar and square

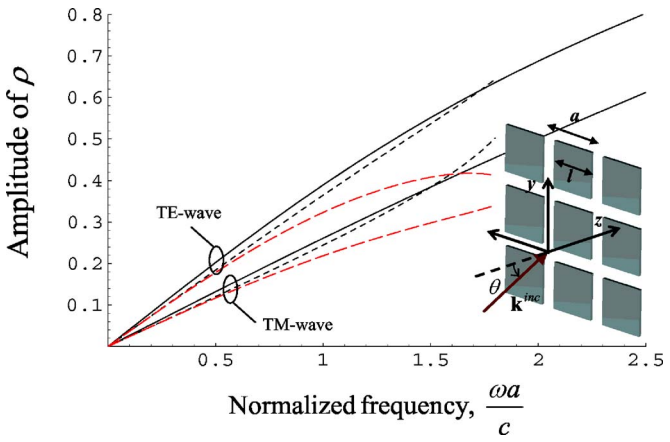

FIG. 15. (Color online) Amplitude of the reflection coefficient as a function of normalized frequency. The incident wave propagates along $\theta=45$ (deg). Solid (black) line: full wave results; dashed (black) line: TA field method; short-dashed (red—light gray in grayscale) line: classical theory. The inset shows the geometry of the metamaterial slab (one layer).

shaped with length $l=0.8a$. This periodic structure is typically modeled as an uniaxial material characterized by an effective permittivity and an effective permeability [21]. The nontrivial components of the effective medium (relative) parameters are $\varepsilon_{\|}\equiv\varepsilon_{xx}=\varepsilon_{yy}$ and μ_{zz}. It is well known that the modal solutions can be classified into TE and TM modes relative to the z direction. The dispersion characteristic of the TE and TM modes is given by

$$k_{z,\mathrm{TM}}^2=(\beta^2-k_{\|}^2)\varepsilon_{\|}, \tag{53}$$

$$k_{z,\mathrm{TE}}^2=\beta^2\varepsilon_{\|}-\frac{k_{\|}^2}{\mu_{zz}}. \tag{54}$$

Even though the magnetization vector $\mathbf{M}$ in the periodic medium is nontrivial, the scattering of waves by a metamaterial slab can still be calculated using Eqs. (36) and (37), as explained in Sec. IV A.

To use Eqs. (36) and (37) we need to know the parameters $\varepsilon_{\|}$ and μ_{zz}. Unfortunately, there is no simple analytical model that allows the calculation of these parameters as a function of frequency. To circumvent this problem, we computed $\varepsilon_{\|}$ and μ_{zz} directly from the band structure of the infinite lattice, using the numerical method introduced in Ref. [26]. We found out that $\varepsilon_{\|}$ increases from 1.7 (static limit) to 2.1 at $\beta a=1.8$, and that μ_{zz} decreases from 0.76 down to 0.70 in the same frequency range. At $\beta a=1.9$ the infinite lattice has a band gap (for propagation along the z direction), and consequently, we do not have data to compute the effective parameters for frequencies above that value.

In Fig. 15 we show the computed reflection coefficient for incidence along $\theta=45$ and $\phi=0$ (deg). It is seen that the TA-field method (dashed black line) agrees well with the full wave results. On the contrary, the classical approach (short dashed red line) starts to fail for relatively small frequencies. This again demonstrates that the new approach proposed in this paper is more accurate and general.

VII. CONCLUSION

The results of this work demonstrate that the classical homogenization approach has important limitations, and in some cases may not be suitable to characterize thin metamaterial slabs for moderately small frequencies. For some configurations the classical approach also fails to predict the cross-polarization level and the reflection properties of the evanescent modes. To circumvent these problems, we generalized the homogenization technique introduced in our previous publication [14]. It was shown that the TA-field method can predict with excellent accuracy the reflection properties of both thin and thick metamaterial slabs in complex setups, even for wide incident angles and evanescent modes. It was explained that in many relevant configurations the TA-fields can be easily related with the bulk medium fields, and consequently, the complexity of the new method is comparable to that of the classic approach. It was demonstrated that for an important class of problems, an additional boundary condition is necessary to properly homogenize the metamaterial slab, and it was also proved that in the long wavelength limit the new method is equivalent to the classic approach. We hope that the theoretical developments presented here shed some light over some important fundamental concepts used in the homogenization of artificial materials, and contribute to a more complete and profound understanding of the phenomenology and electrodynamics of these structures.

ACKNOWLEDGMENTS

This work was funded by Fundação para a Ciência e a Tecnologia under Project No. POSC/EEACPS/61887/2004.

APPENDIX A: CALCULATION OF THE TRANSVERSE AVERAGED FIELDS IN A PERIODIC CRYSTAL

We consider the geometry described in Sec. IV. To calculate the transverse averaged fields it is convenient to write the electromagnetic fields in terms of the polarization currents. Using standard Green function methods [21], it can be proved that the electric field has the following integral representation:

$$\mathbf{E}(\mathbf{r})=\int_{\Omega}\left(\frac{\varepsilon(\mathbf{r}')}{\varepsilon_h}-1\right)\beta^2\bar{\bar{\mathbf{G}}}_p(\mathbf{r}|\mathbf{r}')\cdot\mathbf{E}(\mathbf{r}')d^3\mathbf{r}', \tag{A1}$$

where the primed and unprimed coordinates represent the source and observation points, respectively, $\beta=\omega\sqrt{\varepsilon_h\mu_0}$ is the wave number in the host medium, and the Green function dyadic is defined by

$$\bar{\bar{\mathbf{G}}}_p=\left(\bar{\bar{\mathbf{I}}}+\frac{1}{\beta^2}\nabla\nabla\right)\Phi_p. \tag{A2}$$

In the above, $\Phi_p=\Phi_p(\mathbf{r}|\mathbf{r}')$ is the dynamic potential created by a phase-shifted array of point sources,

$$\nabla^2\Phi_p+\beta^2\Phi_p=-\sum_{\mathbf{I}}\delta(\mathbf{r}-\mathbf{r}'-\mathbf{r}_{\mathbf{I}})e^{-j\mathbf{k}\cdot(\mathbf{r}-\mathbf{r}')}, \tag{A3}$$

where δ is the Dirac function, $\mathbf{I}=(i_1,i_2,i_3)$ is a multi-index of integers, and $\mathbf{r}_I=i_1\mathbf{a}_1+i_2\mathbf{a}_2+i_3\mathbf{a}_3$ is a lattice point.

In order to calculate $\mathbf{E}_{\mathrm{av},T}$, given by Eq. (15), we multiply both sides of Eq. (A1) by $e^{j\mathbf{k}_\parallel\cdot\mathbf{r}}$ and integrate over Ω_T. In this way, we obtain that

$$\mathbf{E}_{\mathrm{av},T}(z) = -j\omega\mu_0 \int_\Omega \overline{\overline{\mathbf{G}_{0,T}}}(z|z')\cdot\mathbf{J}_d(\mathbf{r}')e^{j\mathbf{k}_\parallel\cdot\mathbf{r}'}d^3\mathbf{r}', \quad \text{(A4)}$$

where we defined,

$$\overline{\overline{\mathbf{G}_{0,T}}}(z|z') = \frac{1}{A_{\mathrm{cell}}}\int_{\Omega_T} \overline{\overline{\mathbf{G}_p}}(\mathbf{r}|\mathbf{r}')e^{j\mathbf{k}_\parallel\cdot(\mathbf{r}-\mathbf{r}')}dxdy. \quad \text{(A5)}$$

Quite interestingly, the dyadic $\overline{\overline{\mathbf{G}_{0,T}}}$ can be calculated in closed analytical form. In fact, using the spectral-like representation of $\overline{\overline{\mathbf{G}_p}}$ derived in Ref. [20] (see also Ref. [14]) it is straightforward to obtain Eq. (23). Finally, we can use Eq. (17) in Eq. (A4) to obtain Eq. (22).

APPENDIX B: CALCULATION OF THE TRANSVERSE AVERAGED FIELDS FOR VERY LONG WAVELENGTHS

In this appendix we derive Eqs. (38) and (39). Consider an electromagnetic mode in a periodic crystal, and suppose that the inclusions in the unit cell are electrically small so that, with the exception of the electric and magnetic dipole moments, all the other induced multipole moments can be neglected. Then, to a first approximation, and for generic vector $\mathbf{u}$, we have that

$$\frac{1}{V_{\mathrm{cell}}j\omega}\int_\Omega \mathbf{J}_d e^{j\mathbf{u}\cdot\mathbf{r}}d^3\mathbf{r} \approx \mathbf{P} - \frac{\mathbf{u}}{\omega}\times\mathbf{M}, \quad \text{(B1)}$$

where $\mathbf{P}$ and $\mathbf{M}$ are the polarization and magnetization vectors, respectively [see Eqs. (9) and (10)]. To obtain Eq. (B1) we used the approximation $e^{j\mathbf{u}\cdot\mathbf{r}}\approx 1+j\mathbf{u}\cdot\mathbf{r}$ and the fact that $\frac{1}{V_{\mathrm{cell}}}\int_\Omega \mathbf{u}\cdot\mathbf{r}\mathbf{J}_d(\mathbf{r})d^3\mathbf{r}\approx -\mathbf{u}\times\mathbf{M}$ when the electric quadrupole moment is negligible [16]. In particular, Eq. (B1) shows that the generalized polarization vector given by Eq. (6) satisfies Eq. (8).

Let $\mathbf{k}=(k_x,k_y,k_z)$ be the wave vector of the pertinent electromagnetic mode in the artificial material. The longitudinal component of the wave vector is, of course, k_z. Note that if the dielectric inclusions were removed, the longitudinal component of the wave vector would be $\pm j\gamma_0 = \pm j\sqrt{\mathbf{k}_\parallel\cdot\mathbf{k}_\parallel - \beta^2}$. Let us consider the regime in which $|\gamma_0 a_\perp| \ll \pi$ and $|k_z a_\perp| \ll \pi$. In this regime, A_0 given by Eq. (24) is to a first approximation equal to (since the denominators of the quotients are close to zero)

$$A_0(z;k_z) \approx \frac{1}{2A_{\mathrm{cell}}\gamma_0}\sum_\pm \frac{e^{\pm\gamma_0 z}}{a_\perp(\gamma_0 \pm jk_z)}. \quad \text{(B2)}$$

The formula is valid for $|z| < a_\perp$. Hence, using Eq. (B1) we obtain the result

$$\int_\Omega A_0(z-z';k_z)\mathbf{J}_d(\mathbf{r}')e^{j\mathbf{k}_\parallel\cdot\mathbf{r}'}d^3\mathbf{r}'$$

$$\approx \frac{1}{2\gamma_0}\sum_\pm \frac{e^{\pm\gamma_0 z}}{\gamma_0 \pm jk_z}[j\omega\mathbf{P} - j(\mathbf{k}_\parallel \pm j\gamma_0\hat{\mathbf{u}}_z)\times\mathbf{M}]. \quad \text{(B3)}$$

Both sides can be differentiated with respect to z at the z =const. planes that do not intersect the inclusions, and the approximate identity remains valid for the derivatives at these planes. Hence, using Eq. (A4), we find that at these planes (in the unit cell) we have that

$$\mathbf{E}_{\mathrm{av},T}(z) \approx \frac{\mu_0\omega}{2\gamma_0}\sum_\pm \left[\bar{\bar{\mathbf{I}}} + \frac{1}{\beta^2}\left(-j\mathbf{k}_\parallel + \frac{d}{dz}\hat{\mathbf{u}}_z\right)\left(-j\mathbf{k}_\parallel + \frac{d}{dz}\hat{\mathbf{u}}_z\right)\right]$$

$$\cdot[\omega\mathbf{P} - (\mathbf{k}_\parallel \pm j\gamma_0\hat{\mathbf{u}}_z)\times\mathbf{M}]\frac{e^{\pm\gamma_0 z}}{\gamma_0 \pm jk_z}. \quad \text{(B4)}$$

Since we consider that $|\gamma_0 a_\perp| \ll \pi$, we can replace the factors $e^{\pm\gamma_0 z}$ by unity after the derivatives in z are evaluated. Using also Eq. (16), we obtain that

$$\mathbf{E}_{\mathrm{av},T}(z) \approx \frac{\mu_0\omega}{2\gamma_0}\sum_\pm \frac{1}{\gamma_0 \pm jk_z}\left(\bar{\bar{\mathbf{I}}} - \frac{1}{\beta^2}\mathbf{k}_\pm\mathbf{k}_\pm\right)\cdot(\omega\mathbf{P} - \mathbf{k}_\pm\times\mathbf{M}), \quad \text{(B5)}$$

$$\frac{\mathbf{B}_{\mathrm{av},T}(z)}{\mu_0} \approx \frac{1}{2\gamma_0}\sum_\pm \frac{1}{\gamma_0 \pm jk_z}\mathbf{k}_\pm\cdot(\omega\mathbf{P} - \mathbf{k}_\pm\times\mathbf{M}), \quad \text{(B6)}$$

where we defined $\mathbf{k}_\pm = \mathbf{k}_\parallel \pm j\gamma_0\hat{\mathbf{u}}_z$. After laborious but straightforward calculations these formulas can be considerably simplified. We obtain that

$$\mathbf{E}_{\mathrm{av},T}(z) = \frac{(\beta^2\bar{\bar{\mathbf{I}}} - \mathbf{kk})}{k^2-\beta^2}\cdot\left(\frac{\mathbf{P}}{\varepsilon_h} - \frac{\mathbf{k}}{\omega\varepsilon_h}\times\mathbf{M}\right) + \hat{\mathbf{u}}_z\hat{\mathbf{u}}_z\cdot\frac{\mathbf{P}}{\varepsilon_h}, \quad \text{(B7)}$$

$$\frac{\mathbf{B}_{\mathrm{av},T}(z)}{\mu_0} = \frac{1}{k^2-\beta^2}\mathbf{k}\times(\omega\mathbf{P} - \mathbf{k}\times\mathbf{M}) + \hat{\mathbf{u}}_z\times(\hat{\mathbf{u}}_z\times\mathbf{M}). \quad \text{(B8)}$$

Finally, one can relate the polarization and the magnetization vectors with the bulk medium average fields. Using Eqs. (4), (5), and (8), it is straightforward to demonstrate that the previous formulas simplify to the remarkably simple results Eqs. (38) and (39).

[1] *Metamaterial Structures, Phenomena, and Applications*, edited by T. Itoh and A. A. Oliner, special issue of IEEE Trans. Microwave Theory Tech. **53** (2005).
[2] *Metamaterials*, edited by A. Boardman and V. Shalaev, special issue of J. Opt. Soc. Am. B **23** (2006).
[3] N. Engheta, IEEE Antennas Wireless Propag. Lett. **1**, 10 (2002).
[4] J. B. Pendry, Phys. Rev. Lett. **85**, 3966 (2000).
[5] C. Luo, S. G. Johnson, J. D. Joannopoulos, and J. B. Pendry, Phys. Rev. B **68**, 045115 (2003).
[6] P. A. Belov, Y. Hao, and S. Sudhakaran, Phys. Rev. B **73**, 033108 (2006).
[7] D. R. Smith and J. B. Pendry, J. Opt. Soc. Am. B **23**, 391 (2006).
[8] S. Tretyakov, *Analytical Modeling in Applied Electromagnetics* (Artech House, Norwood, MA, 2003).
[9] C. Simovski (private communication); e-print cond-mat/0606622.
[10] W. Lamb, D. M. Wood, and N. W. Ashcroft, Phys. Rev. B **21**, 2248 (1980).
[11] S. Datta, C. T. Chan, K. M. Ho, and C. M. Soukoulis, Phys. Rev. B **48**, 14936 (1993).
[12] M. Silveirinha and C. A. Fernandes, IEEE Trans. Microwave Theory Tech. **53**, 1418 (2005).
[13] D. R. Smith, S. Schultz, P. Markos, and C. M. Soukoulis, Phys. Rev. B **65**, 195104 (2002).
[14] M. Silveirinha and C. A. Fernandes, IEEE Trans. Antennas Propag. **53**, 59 (2005).
[15] M. Silveirinha, Phys. Rev. B **75**, 115104 (2007).
[16] J. D. Jackson, *Classical Electrodynamics* (Wiley, New York, 1999).
[17] I. V. Lindell, A. H. Sihvola, S. A. Tretyakov, and A. Viitanen, *Electromagnetic Waves in Chiral and Bi-Isotropic Media* (Artech House, Norwood, MA, 1994).
[18] L. Landau and E. Lifchitz, *Electrodynamics of Continuous Media—2nd Ed. Course of Theoretical Physics* (Elsevier Butterworth-Heinemann, 1984), Vol. 8, Chap. 12.
[19] M. Silveirinha, IEEE Trans. Antennas Propag. **54**, 1766 (2006).
[20] M. Silveirinha and C. A. Fernandes, IEEE Trans. Antennas Propag. **53**, 347 (2005).
[21] R. Collin, *Field Theory of Guided Waves* (IEEE Press, Piscataway, NJ, 1990).
[22] P. A. Belov and M. G. Silveirinha, Phys. Rev. E **73**, 056607 (2006).
[23] M. G. Silveirinha, Phys. Rev. E **73**, 046612 (2006).
[24] P. A. Belov, C. R. Simovski, and P. Ikonen, Phys. Rev. B **71**, 193105 (2005).
[25] C. R. Simovski and P. A. Belov, Phys. Rev. E **70**, 046616 (2004).
[26] M. Silveirinha and C. A. Fernandes, IEEE Trans. Microwave Theory Tech. **51**, 1460 (2003).